

Curriculum Vitae

Benjamin A. Portney

bportney@gmail.com

linkedin.com/in/ben-portney

Doctor of Philosophy, 2018

EDUCATION

- 2013-2018 Ph.D. Candidate, Graduate Program in Biochemistry and Molecular Biology
University of Maryland, Baltimore – Baltimore, MD
- 2007-2011 B.S., General Biology
University of Maryland, College Park – College Park, MD
- 2007-2011 Minor, Leadership Studies
University of Maryland, College Park – College Park, MD

RESEARCH EXPERIENCE

- 2013-2018 Graduate Research Assistant, Mentor: Michal Zalzman, Ph.D.
University of Maryland School of Medicine
- 2010 Undergraduate Research Assistant, Mentor: Jack Blanchard, Ph.D.

PUBLICATIONS

Portney, B. A., Khatri, R. Meltzer. W.A., Mariano, J.M., Zalzman, M. (2018) ZSCAN4 is negatively regulated by the ubiquitin proteasome system and the E3 ubiquitin ligase RNF20. *Biochemical and Biophysical Research Communications*, 2018.

Khatri, R., Arad, M., Ortlip, T., **Portney, B. A.**, Meltzer, W. A., Diaconu, S.,... Zalzman, M. (2017). Harvesting multipotent progenitor cells from a small sample of tonsillar biopsy for clinical applications. *Stem Cell Research & Therapy*, 8(1), 174. doi: 10.1186/s13287-017-0619-x

Portney BA, Vanegas C, Hung A, Egbulem C. Exploring Entrepreneurship at the University of Maryland, Baltimore. 2017. *University of Maryland Baltimore*; [ISSUU](#).

SELECTED PRESENTATIONS

GAP Summit

Washington, DC

Georgetown University

June 2017

Poster Presentation: Science Connect! Increasing Science Literacy and Communication One Connection at a Time

**Blanchard/Kleinman Commemorative Lecture Retreat
Baltimore, MD**

University of Maryland School of Medicine

June 2017

Oral Presentation: Embryonic Gene Pathways in Cancer Stemness

6th Annual Biochemistry Retreat

Baltimore, MD

University of Maryland School of Medicine

January 2017

Poster Presentation: ZSCAN4 is Regulated by the Ubiquitin-Proteasome System and Interacts with the E3 ubiquitin ligase RNF20

5th Annual Biochemistry Retreat

Baltimore, MD

University of Maryland School of Medicine

January 2016

Poster Presentation: The Role of ZSCAN4 in HNSCC Cancer Stem Cells

4th Annual Biochemistry Retreat

Baltimore, MD

University of Maryland School of Medicine

January 2015

Poster Presentation: ZSCAN4 is Essential for HNSCC Tumor Development In Vivo

7th Annual Maryland Stem Cell Research Symposium

Silver Spring, MD

Maryland Stem Cell Research Fund

December 2014

Poster Presentation: Expansion and Differentiation Potency of Tonsil Stem Cells

Abstract

The Role of ZSCAN4 in Cancer Stemness

Benjamin A Portney, Doctor of Philosophy, 2018

Dissertation Directed by:

Michal Zalzman, PhD, Assistant Professor
Department of Biochemistry and Molecular Biology
Department of Otorhinolaryngology – Head and Neck Surgery
University of Maryland School of Medicine

Cancer stem cells (CSCs) represent a subset of cells within tumors that maintain the ability to self-renew, drive tumor heterogeneity, and contribute to therapeutic resistance and cancer recurrence. Over the past decade, embryonic factors have emerged as key regulators of cancer stemness and as therapeutic targets. *Zscan4* is an early embryonic gene expressed in mouse embryonic and induced pluripotent stem cells where it plays critical roles in genomic stability, telomere maintenance, and pluripotency. Like other embryonic factors, ZSCAN4 is reactivated in cancer. In these studies, we define for the first time the role of ZSCAN4 in human CSCs of head and neck squamous cell carcinoma (HNSCC). We find that ZSCAN4 is enriched for in and marks the HNSCC CSC population. Induction of ZSCAN4 promotes the CSC phenotype, increases CSC factors and alters the epigenetic profile. Importantly, extreme limiting dilution analyses both *in vitro* and *in vivo* indicate that ZSCAN4 induction significantly increases the frequency of CSC. Consistently, ZSCAN4 depletion leads to loss of the CSC phenotype including CSC marker expression, the ability to form spheroids in non-adherent culture conditions, and hypersensitivity to genotoxic drugs. Furthermore, loss of ZSCAN4 severely impairs tumor growth *in vivo*.

As our findings indicated that ZSCAN4 promotes the CSC phenotype, we next chose to study its regulation and turnover in cancer cells. Expression of *Zscan4* is transient, and characterized by infrequent high expression peaks that are quickly down-regulated, suggesting its expression is tightly controlled. However, little is known about the protein degradation pathway responsible for regulating the human ZSCAN4 protein levels. We first determined the protein half-life of ZSCAN4 and elucidated the role of the ubiquitin proteasome system in ZSCAN4 degradation. Importantly, our data indicate an interaction between ZSCAN4 and the E3 ubiquitin ligase RNF20. RNF20 depletion stabilizes the ZSCAN4 protein half-life, suggesting that RNF20 negatively regulates ZSCAN4 stability. Due to the crucial cellular functions of ZSCAN4, these results have important implications in telomere regulation, stem cell biology, and cancer. Overall, our study suggests that ZSCAN4 plays a critical role in maintaining the undifferentiated state and survival of CSCs, indicating that ZSCAN4 is a potential therapeutic target in HNSCC.

The Role of ZSCAN4 in Cancer Stemness

by
Benjamin A Portney

Dissertation submitted to the Faculty of the Graduate School of the
University of Maryland, Baltimore in partial fulfillment
of the requirements for the degree of
Doctor of Philosophy
2017

Acknowledgements

I would first like to thank my family for their constant love and support. To my mom and dad, Leslie and David, and my sister Jessika, thank you for always being there to listen and offer encouragement. I'd next like to thank my mentor, Dr. Michal Zalzman, for her continuous support (both in and out of the lab). Thank you for your patience, kindness, scientific curiosity, open-mindedness, and mentorship. Special thanks to Dr. Karen Avraham, for connecting me with Dr. Zalzman and offering her guidance. Thank you also to my committee members, Drs. Drohat, Karbowski, Kaetzel, Passanniti, and Starz-Gaiano for their expertise and helpful feedback. I would like to thank the Biochemistry and Molecular Biology Department graduate program for providing me with the learning environment I needed to grow as a scientist. To my program director Dr. Gerald Wilson, thanks for being there to listen and offer words of wisdom. Additional thanks to our department front office, in particular Koula, Kathleen, Taylor, and Heather for their friendship and support. I have been fortunate to work in a great lab with wonderful members: Drs. Alex Meltzer, Raju Khatri, Michal Arad, Aditi Gupta, as well as all medical residents and rotation students I've worked with. It was a pleasure working with all of you. Thanks also to the Kaetzel, Eckert, and Hornyak labs, especially Drs. Katie Leonard, Emmanuel Kalapurakal, and Guatam Adhikary, for their assistance. I am grateful to my many mentors Drs. Darryl Carter, Ken Malone, Martha Connelly, and Mark Lafferty, who took the time to support me and my career interests. Thank you to all of my graduate school friends who made school fun and exciting. I would also like to thank all of my friends and extended family members who supported me throughout my time here. Last, but certainly not least, thank you to Sarah, je t'aime.

Table of Contents

Table of Contents	
Chapter 1: Introduction	1
1.1 ZSCAN4	1
1.1.1 ZSCAN4 in Mouse Embryonic Stem Cells	1
1.1.2 ZSCAN4 in Induced Pluripotent Stem Cells	3
1.1.3 ZSCAN4 in Cancer	4
1.2 Cancer Stem Cells	5
1.2.1 Tumor Heterogeneity	5
1.2.2 CSC Background	7
1.2.3 Identifying CSCs	8
1.2.4 Molecular Pathways of CSCs	9
1.2.5 CSCs and Metastasis	12
1.2.6 CSCs and Drug Resistance	13
1.2.7 Implications of CSCs in cancer therapy	14
1.3 Head and Neck Squamous Cell Carcinoma	16
1.3.2 CSCs in Head and Neck Squamous Cell Carcinoma	17
1.4 Protein Turnover	19
1.4.1 Autophagy	20
1.4.2 The Ubiquitin Proteasome System	22
1.4.3 The E3 ubiquitin ligase RNF20	25
1.5 Scope of Work	26
Chapter 2: ZSCAN4 promotes survival and growth of head and neck squamous cell carcinoma stem cells	28
2.1 Introduction	28
2.2 Materials and Methods	30
2.3 Results	35
2.3.1 ZSCAN4 is highly expressed in a fraction of HNSCC cells	35
2.3.2 ZSCAN4 marks tumorsphere forming cells in HNSCC	37
2.3.3 ZSCAN4 expression promotes the CSC phenotype	39

2.3.4 ZSCAN4 induction facilitates chromatin remodeling	39
2.3.5 ZSCAN4 induction increases tumorsphere formation ability <i>in vitro</i> and the frequency of CSC derived tumors <i>in vivo</i>	42
2.3.6 ZSCAN4 is required for maintenance of the CSC phenotype and tumorsphere formation.....	46
2.3.7 ZSCAN4 depletion leads to hypersensitivity to genotoxic drugs.....	48
2.3.8 ZSCAN4 depletion severely affects tumor growth	49
2.4 Discussion.....	50
Chapter 3: ZSCAN4 is negatively regulated by the ubiquitin-proteasome system and the E3 ubiquitin ligase RNF20	54
3.1 Introduction	54
3.2 Materials and Methods	56
3.3 Results	60
3.3.1 ZSCAN4 protein turnover and half-life	60
3.3.2 ZSCAN4 degradation is proteasome dependent.....	62
3.3.3 ZSCAN4 is marked for proteasomal degradation by lysine 48 ubiquitination	65
3.3.4 The E3 ubiquitin ligase RNF20 negative regulates ZSCAN4 protein stability	67
3.4 Discussion.....	70
Chapter 4: Conclusions, Perspectives, and Future Directions	72
4.1 Conclusions	72
4.2 Outstanding Questions and Future Directions	73
4.2.1 How is ZSCAN4 expression regulated in CSCs?	73
4.2.2 How does ZSCAN4 facilitate an open chromatin state?	74
4.2.3 Is ZSCAN4 activity on telomeres mediated through its epigenetic effect on telomeric chromatin?	75
4.2.4 Is ZSCAN4 involved in DNA repair?	76
References.....	77

List of Figures

Figure 1.1 Tumor heterogeneity models.....	6
Figure 1.2 Implications of CSCs in cancer therapy	15
Figure 1.3 Schematic of Autophagy	22
Figure 1.4 The Ubiquitin Proteasome System	24
Figure 2.1 Expression of ZSCAN4 is upregulated in human head and neck cancers	36
Figure 2.2 ZSCAN4 marks cancer stem cells in HNSCC	38
Figure 2.3 Induction of ZSCAN4 promotes the cancer stem cell phenotype	41
Figure 2.4 ZSCAN4 increases tumorsphere formation.....	44
Figure 2.5 ZSCAN4 increases CSC frequency and tumor formation.....	45
Figure 2.6 ZSCAN4 is required for the expression of cancer stem cell markers	46
Figure 2.7 ZSCAN4 is essential for tumorsphere growth and survival.....	47
Figure 2.8 ZSCAN4 Depletion leads to hypersensitivity to genotoxic drugs.....	49
Figure 2.9 ZSCAN4 depletion severely affects tumor growth	50
Figure 3.1 Human ZSCAN4 protein half-life and cellular localization.....	62
Figure 3.2 ZSCAN4 degradation is proteasome dependent.....	64
Figure 3.3 ZSCAN4 is ubiquitinated on Lysine 48 (K48Ub).....	66
Figure 3.4 The E3 ubiquitin ligase RNF20 negatively regulates and interacts with ZSCAN4	69

List of Tables

Table 2.1 List of Antibody Dilutions	33
--	----

List of Abbreviations

ABC	ATP binding cassette
ABCG2	ATP binding cassette subfamily G member 2
ALDH1	Aldehyde Dehydrogenase 1
AML	Acute myeloid leukemia
AMPK	Adenosine monophosphate-activated protein kinase
ANOVA	Analysis of variance
ATG	Autophagy related gene
ATP	Adenosine tri phosphate
BCL-2	B-cell lymphoma 2
BCL-XL	B-cell lymphoma-extra large
BMI-1	B lymphoma mo-MLV insertion region 1
BLM	Bleomycin
BRE1	Ring finger protein 20, E3 ubiquitin protein ligase
CAM	Chaperone mediate autophagy
CD	Cluster of differentiation
CE	Clonal evolution
ChIP	Chromatin immunoprecipitation
CHX	Cyclohexamide
CPT	Cisplatin
CSC	Cancer stem cell
DNA	Deoxyribonucleic acid
DNMT	DNA methyltransferase
DMEM	Dulbecco's modified eagle medium
DMSO	Dimethyl sulfoxide

Dox	Doxycycline
ECL	Enhanced chemiluminescence
EMT	Epithelial mesenchymal transition
ELDA	Extreme Limiting Dilution Assay
ES cell	Embryonic stem cell
EZH2	Enhancer of zeste homolog 2
FACT	Facilitates chromatin transcription
GFP	Green fluorescent protein
H2Bub1	Histone 2B monoubiquitinated
HDAC	Histone deacetylase
HECT	Homologous to the E6-AP Carboxyl Terminus domain
HNSCC	Head and neck squamous cell carcinoma
HPV	Human papilloma virus
IP	Immunoprecipitation
iPS cell	Induced pluripotent stem cell
JAK	Janus kinase
kDA	kilo Dalton
KLF4	Kruppel like factor 4
LC3	Light chain 3 alpha
LER	Leucine rich region
Lys	Lysine
mDA	mega Dalton
MDR1	Multidrug resistance protein 1
mES cell	Mouse embryonic stem cell
MG132	Carbobenzoxy-Leu-Leu-leucinal

MMC	Mitomycin c
MRE11A	Meiotic recombination 11 homolog a
mTOR	Mammalian target of rapamycin
MTT	3-(4,5-dimethylthiazol-2-yl)-2,5-diphenyltetrazolium bromide
MYC	Myelocytomatosis viral oncogene
NF-kB	Nuclear factor kappa b
NSG	NOD scid gamma
NTC	Non-template control
OCT4	Octamer-binding transcription factor 4
PAF	Platelet activating factor
PBS	Phosphate buffered saline
PI3K	Phosphoinositide 3-kinase
PTEN	Phosphatase and tensin homolog
PVDF	Polyvinylidene difluoride
qRT-PCR	Quantitative reverse transcription polymerase chain reaction
RAD50	DNA repair protein RAD50
RING	Really interesting new gene-finger
RIPA	Radioimmunoprecipitation assay buffer
RNA	Ribonucleic acid
RNF20	Ring-finger protein 20
RPLPO	Large ribosomal protein
RPM	Revolution per minute
SEM	Standard error of the mean
shRNA	Short hairpin RNA
siRNA	Small interfering RNA

SOX2	Sex determining region Y Box-2
STAT	Signal transducer and activator of transcription
TBS	Tris buffered saline
TBST	Tris buffered saline and tween 20
TCL	Total cell lysate
Ub	Ubiquitin
UPS	Ubiquitin-proteasome system
ULK1/2	Unk-51 like autophagy activating kinase 1/2
USP22	Ubiquitin specific peptidase 22
Wnt	Wingless-type MMTV (mouse mammary tumor virus) integration site
WT	Wild type
ZSCAN4	Zinc finger scan domain containing 4

Chapter 1: Introduction

1.1 ZSCAN4

Zscan4 is an embryonic gene implicated in preservation of potency, telomere elongation, and genomic stability [1]. Initially discovered in the mouse, ZSCAN4 is a nuclear protein expressed exclusively during the 2 cell stage (8 cell stage in human) of preimplantation development *in vivo*. ZSCAN4 expression is essential for preimplantation development as knockout experiments delay progression from the 2 cell to the 4 cell stage [2].

Appropriately named for its structure, ZSCAN4 (zinc finger and scan domain containing-protein 4) encodes an N-terminal SCAN domain linked to four zinc finger domains. SCAN domains, also called “leucine rich regions” (LERs), are highly conserved motifs found in the C₂H₂ subfamily of zinc finger proteins and function in protein-protein interactions [3]. Zinc finger domains, short 30 amino acid sequences with secondary structure stabilized by a zinc ion, are present in a broad class of versatile nucleic acid recognition and binding proteins [4].

Consistent with its structure, ZSCAN4 has been demonstrated to both bind DNA and interact with other proteins. The majority of ZSCAN4 studies have been completed in mice. However, the murine and human ZSCAN4 share 78% homology in conserved regions, suggesting similar function between species.

1.1.1 ZSCAN4 in Mouse Embryonic Stem Cells

ZSCAN4 is expressed heterogeneously in mouse embryonic stem (mES) cells *in vitro* [5]. mES cells are derived from the inner cell mass of murine blastocysts. They are

unique in that they exhibit both unlimited self-renewal and pluripotent differentiation, both of which ZSCAN4 has been shown to be a contributing factor [6].

ZSCAN4 has primarily been studied in relation to mES cell long term self-renewal potential through its facilitation of telomere elongation. Expression of ZSCAN4 is associated with recovery of shortened telomeres, achieved through increased telomeric recombination [7]. Further, ZSCAN4 localizes to telomeric DNA and interacts with meiotic DNA repair proteins. Loss of ZSCAN4 results in mES cell telomere shortening that eventually leads to culture crisis. Importantly, ZSCAN4 mediated telomere elongation is independent of telomerase activity, suggesting a novel mechanism for telomere elongation [1].

mES cell pluripotent differentiation potential is maintained through expression of a network of pluripotency genes, facilitated by a decondensed chromatin state [8]. Remarkably, ZSCAN4 expression “bursts” are associated with a global derepression of chromatin to a more open, euchromatic state. These bursts are associated with increased open chromatin marks such as histone acetylation [9]. Unsurprisingly, ZSCAN4 expression improves the developmental potency of mES cells, likely through its activation of other genes expressed during the two cell stage [10]. A recent study demonstrated that the epigenetic impact of ZSCAN4 goes beyond pluripotency preservation as ZSCAN4 expression inhibited DNA methylation maintenance in order to facilitated mES cell telomere elongation [11].

Interestingly, mES cell expression of ZSCAN4 is transient, with only 5% of mES cells expressing ZSCAN4 at any given time. Ultimately, every mES cell in culture will activate ZSCAN4 [1]. Transient ZSCAN4 expression is characterized by short term

“bursts” that quickly subside, suggesting it is tightly controlled at the transcript level [9]. ZSCAN4 expression can also be triggered through a DNA damage response caused by telomere shortening or DNA damage [12]. Recent evidence suggests ZSCAN4 expression is unique to a small and transient population of totipotent mES cells in long-term culture [9]. ZSCAN4 is also regulated at the protein level and has a half-life ranging up to 6 hours [12]. However, little else is known about the mechanisms involved in ZSCAN4 protein turnover.

1.1.2 ZSCAN4 in Induced Pluripotent Stem Cells

Induced pluripotent stem (iPS) cells represent a relatively new type of pluripotent and immortal stem cell. iPS cells are artificially reprogrammed or “induced” back from differentiated adult cells to an immortal embryonic state capable of pluripotent differentiation [13]. Therefore, iPS cells have tremendous potential in regenerative medicine, disease modeling, and drug discovery. The utility of ZSCAN4 has repeatedly been demonstrated in iPS cells.

iPS cells were first developed in mice through the addition of 4 transcription factors (OCT4, SOX2, KLF4, cMYC) by Yamanaka (subsequently called Yamanaka factors, or the core pluripotency factors). These cells were plagued by genomic instability showing gene duplications, deletions and chromosomal abnormalities. Addition of ZSCAN4 to the four Yamanaka factors drastically reduces genomic instability caused by the DNA damage response and increases iPS cell generation [14]. iPS cells generated with ZSCAN4 along with Yamanaka factors were shown to have longer telomeres and generated iPS cell derived live born mice at a higher rate compared to cells generated from Yamanaka factors alone. Further studies demonstrate that addition of ZSCAN4 to

the Yamanaka factors results in the induction of pre-implantation specific genes and greatly improve iPS cell quality, as shown by OCT4 expression. ZSCAN4 can even replace MYC, which is thought to be responsible for genomic instability, as a Yamanaka factor [15].

1.1.3 ZSCAN4 in Cancer

Human ZSCAN4 has been understudied in comparison to its mouse homolog. Nonetheless, studies have suggested it plays a role in human cancer for multiple reasons [1, 16]. Cancers share many similarities with embryonic stem cells, including their immortality and pluripotent gene expression signatures. While maintenance of telomere length in cancer cells has been mainly accredited to the enzyme telomerase, alternative lengthening mechanisms have been demonstrated [17, 18]. Based on studies from mES cells, ZSCAN4 was suggested to play a role in telomere lengthening in cancer. Furthermore, the ability of ZSCAN4 to activate early embryonic genes matches the role that reactivated pluripotent factors play in cancer [19].

Recent unpublished data from the Zalzman laboratory has indeed demonstrated that ZSCAN4 is re-activated in a range of cancers. Further evidence demonstrates that ZSCAN4 expression is required for telomere maintenance and subsequently cancer cell lifespan [20]. Due to its inactivation after embryogenesis, ZSCAN4 appears to be a bona fide cancer target.

1.2 Cancer Stem Cells

1.2.1 Tumor Heterogeneity

Tumors are a highly heterogeneous tissue. Within a tumor, cells display a wide range of phenotypic and functional differences, complicating both diagnosis and treatment [21, 22]. Genetic and epigenetic variations, as well as variety in biochemical processes, proliferative ability, marker expression, and response to therapy all contribute to tumor heterogeneity [23]. Two models have predominantly been used to explain tumor heterogeneity: the clonal evolution model and the cancer stem cell model [22].

The clonal evolution model (CE), also known as the stochastic model, theorizes that increasing genomic instability and proliferation generate a heterogeneous population of cancer cell that constantly acquire new mutations [24, 25]. An ongoing process of Darwinian evolution selects for the best fit variants within the tumor environment. Multiple subclonal populations throughout the tumor are constantly selected for, driving tumor progression and heterogeneity [22].

The cancer stem cell (CSC) model describes a hierarchy of tumor cells similar to normal tissue. In normal tissue, stem cells represent a rare, slow growing, and self-renewing population capable of differentiation into progenitor and terminally differentiated cells [23, 26]. Like normal tissue stem cells, CSCs represent a rare population within the tumor capable of self-renewal and differentiation into mature tumor cells. In the CSC model, the slow growing CSCs give rise to the rapidly dividing bulk tumor population. The various stages of differentiation arising from the CSCs result in tumor heterogeneity and development [27]. Unlike in the CE model, CSCs can be

identified and selected for, based on their unique properties. In principle, one CSC is capable of giving rise to a new heterogeneous tumor.

However, the CE and CSC models are no longer considered mutually exclusive, as tumor heterogeneity can be due to selection of CSC variants at different stages of differentiation. Moreover, the CSC model has recently moved away from a strict hierarchy to a more dynamic model where bulk tumor cells are capable of dedifferentiation into a “CSC state” in response to cues from the tumor environment [21, 23, 28].

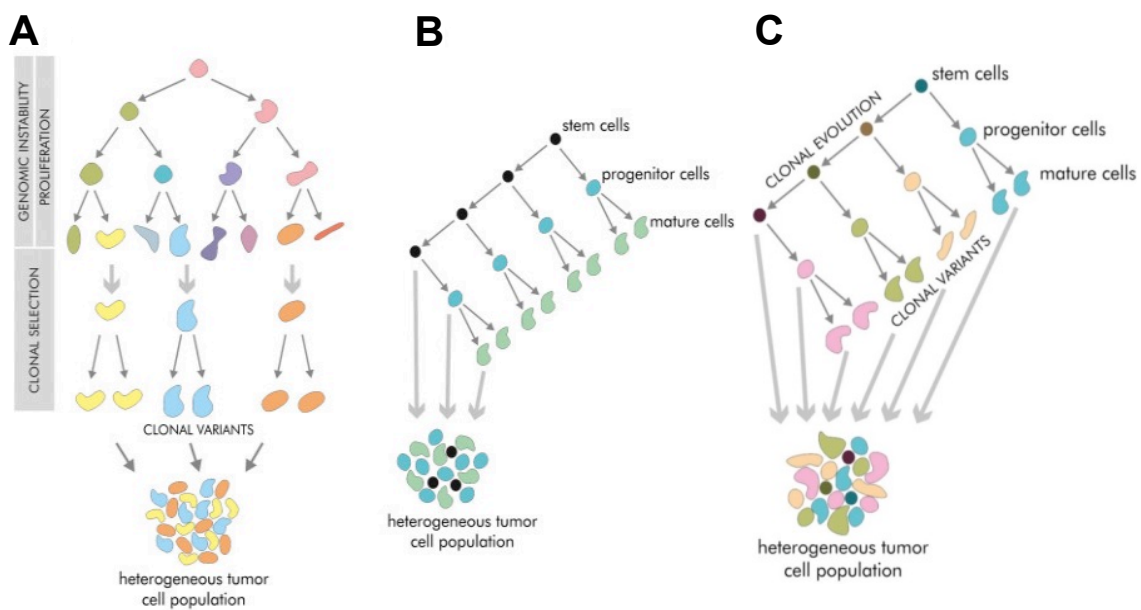


Fig 1.1 Tumor Heterogeneity Models (Adapted from Fulawka, et al., Biol Res, 2014) **A**, Clonal Evolution model. **B**, Cancer Stem Cell model **C**, Hybrid CE and CSC model

1.2.2 CSC Background

Experimental evidence throughout the early to mid-20th century identified many cancers containing slow cycling, highly tumorigenic cells that could differentiate into non tumorigenic types [29]. These cells were linked to normal tissue stem cells and thought to account for tumor heterogeneity, treatment resistance, and cancer recurrence. However, after cancer was established as a genetic disease in the 1970s, tumor heterogeneity was predominantly explained by the CE model [30].

The CSC field reemerged in the mid-1990s when Dick and colleagues demonstrated a distinct subpopulation of primary human acute myeloid leukemia (AML) cells could be propagated in mice. Only the CD34⁺CD38⁻ fractions, the same marker of hematopoietic stem cells, could engraft and lead to AML. Furthermore, this tumor initiating population was extremely rare, at a frequency of one cell per million [31]. Discovery of leukemia CSCs prompted research into other cancer types. The first CSCs defined in solid tumors were in breast cancer by Al Hajj et al [32]. Similar to AML, breast cancer tumors were found to be a heterogeneous population with a rare portion of cells capable of initiating a tumor after serial xenotransplantation into mice. As few as 100 CD44⁺/CD24⁻ cells were capable of recapitulating a tumor, while other phenotypes, even in high numbers, were not. Since then, CSCs have been discovered in a variety of cancers including brain, colon, lung, prostate, head and neck, melanoma, and ovarian [33-39].

In order to generate a universal definition for cancer stem cells, the American Association for Cancer Research convened a CSC workshop in 2006. The workshop's definition stated that, similar to normal tissue stem cells, CSCs represent of subset of the

tumor cells that have the capacity to self-renew and differentiate into a heterogeneous tumor [40]. Also discussed were appropriate markers, experimental assays, and molecular pathways responsible for CSCs, which are presented in more detail below.

1.2.3 Identifying CSCs

According to the CSC hypothesis, CSCs can be isolated based on identifying characteristics and markers. Cell surface antigens and intracellular proteins have been used in a variety of cancers as selection markers for CSCs, often in combination.

Hematological CSCs have typically been identified and isolated using CD34 and CD38 cell surface markers [41]. Two prominent CSC markers in solid tumors include CD44 and CD133. CD44, which is typically expressed in normal mesenchymal stem cells, has been established as a CSC marker in breast, colon, head and neck, liver, and prostate cancer [32, 34, 37, 42-44]. Likewise, CD133 has been used as a marker in colon and prostate cancer, as well as in brain and lung cancers [33, 45-47]. Other CSC cell surface markers such as CD24, CD90 have been used in a variety of cancers [48, 49]. By using antibodies directed to these cell surface antigens, CSC populations can be selected and enriched for experimentally. Intracellular proteins like transcription factors and signaling pathway markers related to CSC function are often upregulated and can be used as markers as well, though are more difficult to select for.

Cancer stem cell markers also include proteins that can be identified and selected for through functional assays. Aldehyde Dehydrogenase (ALDH1) is a detoxifying enzyme found to be upregulated in CSCs of multiple cancers. Cell populations with high ALDH1 activity, as measured by the Aldefluor assay, can be selected for [50]. Another protein upregulated in CSCs, ATP-binding cassette (ABC) transporter proteins, can

rapidly efflux drugs and fluorescent dyes. The side population assay allows detection of CSC fractions based on dye efflux measured by flow cytometry [51]. Due to their ability to self-renew, CSCs can be also enriched for through *in vitro* spheroid formation assays. Under non-adherent culture conditions with supplemented media, CSCs are capable of proliferation, forming clonal three dimensional spheres, while the more differentiated, bulk tumor population is unable to do so [52].

The defining trait of CSCs is their ability to propagate and form a tumor *in vivo*. The gold standard assay in identifying CSCs from tumors is via serial xenotransplantation into an animal model. CSCs are selected for by the above markers, xenografted into immunocompromised mice and monitored for tumor formation. In order to demonstrate self-renewal, cells are serially isolated from the tumor and grafted into a new mouse [40]. A bulk tumor cell will not be able to recapitulate a tumor while a selected for CSC can develop into a differentiated and heterogeneous tumor. Many assays serially dilute the injected cells in order to determine CSC frequency.

1.2.4 Molecular Pathways of CSCs

CSCs share the same defining qualities as normal stem cells in that they can self-renew and differentiate, albeit abnormally. Expectedly, CSCs utilize signal transduction, transcriptional, and epigenetic pathways that are typically attributed to adult and embryonic stem cells. Adoption of these stem like programs accounts for CSC tumorigenesis, metastasis, and treatment resistance.

Developmental signaling pathways such JAK/STAT, Notch, Wnt, and Hedgehog are highly active in CSCs. Cross-talk between these complex pathways occurs regularly in order to regulate and promote the CSC phenotype [53]. Stimulation of JAK proteins by

ligand binding results in association and activation of STAT regulated self-renewal and neurogenesis [54]. JAK/STAT signaling and associated gene activation has been shown to be highly upregulated in the CSC fraction of breast and prostate cancers [55, 56]. The Notch pathway assists in normal stem cell proliferation and cell-fate determination and has also been implicated several cancers [57]. The Wnt pathway, a highly conserved pathway involved in tissue homeostasis and embryonic development, was demonstrated to play a role in regulating CSCs of many cancers, including blood and breast [58, 59]. Another pathway essential for proper development during embryogenesis is the hedgehog pathway. Aberrant Hedgehog activity has also been reported in CSC populations [60]. Other pathways like the PI3K/PTEN and NF- κ B were shown to be dysregulated in CSC populations [61, 62]. Additional signals from the tumor microenvironment, like extracellular matrices, somatic cells, and the vasculature, contribute to activation of CSC pathways [63].

Pluripotent transcription networks stimulated by signaling pathways also promote the CSC state. Indeed, there is a strong link between pluripotency and tumorigenesis, as embryonic stem cells inherently have tumorigenic potential [64]. The core transcriptional circuitry that maintains pluripotent stem cells is regulated by transcription factors POU5F1/OCT4, SOX2, and NANOG, all of which have been implicated in CSCs. These master regulators are essential as they synergistically bind their target promoters, generating an additive effect [65]. Oral cancer CSCs enriched for through spheroid assay expressed high levels of OCT4 while SOX2 is highly expressed in melanoma stem cells [66, 67]. NANOG is also expressed in high levels in CSC populations of several cancers [68-70]. Pluripotent factors outside the core network, such as pluripotency

reprogramming factor KLF4, have also been reported to play a role in maintaining CSC populations [71]. As evidence of their role in cancer stemness, elevated expression of pluripotency factors have become markers for CSCs [72].

In order to accommodate stem cell like transcriptional networks, CSCs must also change their epigenetic state [72]. Epigenetics refers to alterations in gene expression without direct changes made to the DNA sequence. This is accomplished through mechanisms including histone modifications, DNA methylation, and non-coding RNAs. Epigenetic changes have previously been linked to cancer and CSCs. Like in embryonic stem cells, global histone acetylation and a subsequent open chromatin state seem critical for CSC viability, as depletion of histone deacetylating enzymes reduces CSC numbers in head and neck cancers [73, 74]. Other histone modifiers responsible for repression of specific pro differentiation genes, such as the Polycomb group proteins, have been shown critical in maintaining cancer stemness. Indeed, Polycomb group proteins BMI-1 and EZH2 serve as CSC markers in squamous cell carcinomas [75, 76]. DNA methylation is also critical for CSCs and global hypomethylation is important for cancer development. DNA methylating enzymes are upregulated in multiple cancers and have been reported to promote CSC maintenance in colorectal cancer [77]. Non-coding RNAs like microRNAs and long non-coding RNAs have been demonstrated in promoting the CSC phenotype as well [78, 79]. Due to their extensive role in CSCs and tumorigenesis, inhibitors of chromatin and DNA modifying enzymes like DNMTs, HDACs, and EZH2 are currently used in the clinic [80, 81].

1.2.5 CSCs and Metastasis

Metastasis is the process by which cancer cells spread from the primary tumor to form secondary tumors at distant sites. Critical to the process is a program where epithelial cells transit to a mesenchymal state, called the epithelial-mesenchymal transition (EMT). The EMT program normally occurs during embryogenesis when epithelial cells lose their polarity in order to migrate and form new tissues, or in adults, during tissue repair. Reactivation of the EMT program has recently been linked to acquisition of the CSC state [82]. Additionally, many similar pathways reactivated in CSCs, such as developmental signaling programs and pluripotent transcription, have also been implicated in EMT [83, 84]. *In vitro*, CSCs possess enhanced invasion and migration abilities compared to bulk tumor cells, as assessed by scratch migration and trans-membrane invasion assays [85].

The mesenchymal phenotype displays increased migratory ability and EMT plays a role in many of the five steps of metastasis: invasion, intravasation, transport, extravasation, and colonization. During invasion of the surrounding tissues, EMT supports the degradation of the extracellular matrix and cellular junctions [86]. As the migrating cells enter the blood and lymph vasculature during the intravasation step, cells that have gone through EMT are capable of releasing proteases to allow transmigration through the basement membrane [87]. Cancer cells of the CSC and mesenchymal phenotype are more capable of surviving transport throughout circulation. Extravasation, or penetration of the basement membrane of distant tissues, has been reported to utilize similar pathways upregulated in CSCs [88]. The final step of metastasis requires enough genomic plasticity to reverse the EMT process and colonize the secondary tissue.

Evidence suggests that CSCs are inherently plastic enough to occupy and initiate a new tumor in distant sites, whereas bulk tumor cells are not [89].

1.2.6 CSCs and Drug Resistance

While treatment options for patients continue to improve, cancer still accounts for 20% of all deaths in developed countries [90]. In various cancers, therapeutic resistance and treatment failure has been attributed to CSCs. Many highly active developmental and signal transduction pathways involved in self-renewal and metastasis confer drug resistance attributes. Conventional cancer therapies target rapidly dividing cells actively engaged in the cell cycle. However, it has been suggested that CSCs are intrinsically slow-growing and quiescent, and can therefore evade elimination [91].

Additionally, compared to bulk tumor cells, CSCs have developed a number of molecular mechanisms to resist conventional anti-cancer therapies like chemotherapy and radiation. Drug efflux pumps are not just CSC markers but contribute to therapeutic resistance. In normal tissues, transporters are expressed in low amounts and protect cells from toxins. In cancer, however, drug efflux pumps such as MDR1 and ABCG2 are upregulated and may facilitate the removal of genotoxic drugs from the cell [92]. Another CSC marker, Aldehyde Dehydrogenase activity, has been shown to protect cells from oxidative stress caused by genotoxic agents [93].

Cancer stem cells also upregulate anti-apoptotic proteins that confer resistance to therapy. For example, quiescent leukemic stem cells were shown to highly express the anti-apoptotic proteins BCL-2 and BCL-XL [94]. As genotoxic drugs and radiation damage the DNA of cancer cells, CSCs have upregulated the DNA damage and repair

response. In glioma, CD133⁺ CSCs were more resistant to ionizing radiation and had increased phosphorylation/activation of DNA damage response factors like ATM [95].

1.2.7 Implications of CSCs in cancer therapy

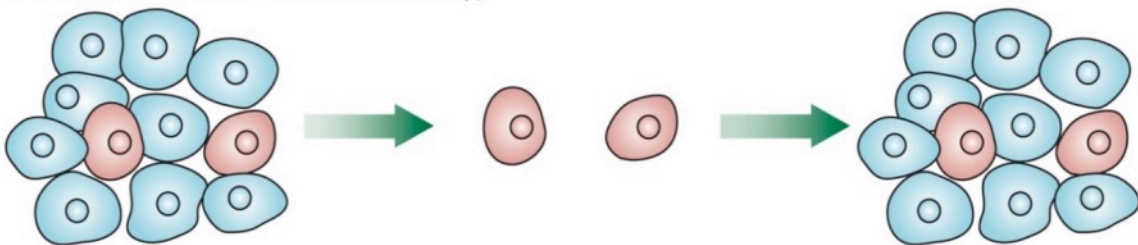
The existence of CSCs has substantial implications for cancer therapy. The CSC theory suggests that CSCs are responsible for treatment resistance and tumor recurrence as they survive conventional therapies like chemotherapy and radiation. New evidence further indicates that traditional therapies induce selection pressure and thereby may enrich for CSCs and increase in invasiveness and malignancy [96]. Accordingly, CSCs have become major targets for drug design both in the lab and clinic [97].

While many molecular pathways protect CSCs from therapeutic intervention and promote metastasis, they can also be exploited as CSC targets. Inhibition of CSC dependent pathways like JAK/STAT, Wnt, Notch, and Hedgehog depletes self-renewal and metastatic capabilities [98]. Several small molecule inhibitors have been identified and developed, with many candidates entering clinical trials [99-101]. Sensitizing drug resistant CSCs to current therapies can be achieved through inhibition of drug efflux pumps and impairment of DNA repair pathways [102, 103]. CSC directed therapies also target metastasis through inhibition of vascularization and disruption of CSC interactions within the tumor microenvironment [104, 105]. Inhibition of epigenetic enzymes like HDACs and EZH2 seeks to restore differentiation programs silenced in CSCs and induce differentiation [76, 106]. Additionally, the growing field of immunotherapy harnesses the immune system to recognize and kill the CSC population based on cell surface marker expression [107]. New therapies must avoid off target toxicity in normal tissue stem cells, as CSCs share many of the same pathways. Therefore, discovery of specific molecular

markers and dissection of novel CSC pathways will allow for more efficient CSC targeting.

Targeting the CSC population alone has the potential to treat many cancers. However, multi-modal therapies that include CSC targeting along with conventional genotoxic therapy to remove bulk tumor cells are becoming the standard of care [108]. Elimination of rapidly dividing bulk tumor cells through chemotherapy or radiation decreases tumor burden while simultaneous targeting of CSCs may further prevent recurrence and metastasis. Moving forward, therapies that go after multiple CSC targets, along with genotoxic therapy, hold potential to improve patient outcomes [109]. Therefore, a better understanding of the CSC phenotype and the contributing pathways are important for new drug discoveries.

A Hierarchic CSC model—conventional therapy



B Hierarchic CSC model—CSC-specific therapy

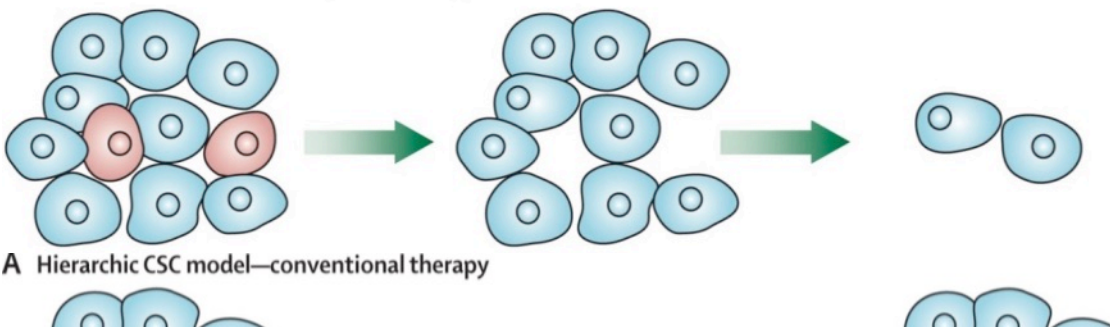


Figure 1.2 Implications of CSC's in cancer therapy (Adapted from Vermeulen et al., *Lancet Oncol*, 2012) **A**, Conventional therapies are unable to kill CSCs, leading to relapse. **B**, CSC specific therapies kill CSCs, preventing relapse.

1.3 Head and Neck Squamous Cell Carcinoma

Cancers arising from squamous epithelium lining the mucosal surfaces of the head and neck region are considered head and neck squamous cell carcinoma (HNSCC) [110]. With presentation at distinct anatomic sites of the head and neck, including the esophagus, pharynx, larynx, and oral and nasal cavities, HNSCC is a complex and heterogeneous disease. As such, HNSCC, the sixth most prevalent cancer globally, poses a major public health concern [111]. In the US alone, HNSCC constitutes approximately fifty thousand new diagnoses and ten thousand deaths per year. The most important risk factors include tobacco use, alcohol consumption, and infection with human papilloma virus (HPV) [112]. Age is also a factor, as cancer rates remain low in children and young adults, and peak after 50 years of age [113].

HNSCC is a progressive disease with tumors developing in multiple stages of pathogenesis [114]. Throughout development, tumor cells accrue epigenetic and genetic mutations, such as amplifications, deletions, rearrangements and point mutations, which result in changes in protein expression [114, 115]. Accumulation of mutations, duplications and deletions in oncogenes and tumor suppressors leads to dysfunction in multiple cellular pathways. Alterations in pathways including cell cycle checkpoints, proliferation, differentiation, survival, invasion and migration have been identified in HNSCC [112].

Tumor staging, determined by the extent of the tumor, if it has spread to nearby lymph nodes, and level of metastasis is an important prognostic factor that generally determines treatment options [116]. Early detection holds a better prognosis; however, only about one third of patients present with early stage disease. Most HNSCC patients

present with later stage disease that has already metastasized to the lymph nodes [117]. Considering all stages together, only 50% of HNSCC patients survive beyond 5 years [118].

Recent advances in single modality treatments like surgery and localized radiotherapy have improved outcomes of early stage patients [119]. Multimodal approaches combining surgery, radiotherapy, and chemotherapy are currently used to treat locally advanced HNSCC [120]. Patients with recurrent and metastatic disease, where surgery is no longer an option, are often placed on regimens of palliative chemotherapy [110]. Novel, patient specific drugs, based on tumor profile have begun to enter the clinic, such as EGFR inhibitors and antibodies [121]. As more HNSCC related genes and pathways are identified, targeted therapies will increasingly enter the clinic. However, survival of more advanced cancers remains low due to local recurrence and more distant metastases.

1.3.2 CSCs in Head and Neck Squamous Cell Carcinoma

A subpopulation of cancer stem cells within HNSCC was first identified in 2007 by Prince et al [37]. Since then, the role of CSCs in head and neck cancer carcinogenesis has been established. HNSCC CSC specific markers and pathways have been discovered within primary tumor samples and among cell lines, allowing further studies into key regulators and novel therapeutic interventions.

The first marker used to identify and isolate HNSCC CSCs was CD44. CD44 expression negatively correlates with overall survival in oral cancers while CD44⁺ cells isolated from tumors are capable of self-renewal and serial xenotransplantation [122]. Subsequent HNSCC CSC specific surface markers have been discovered including CD10

and CD133, both of which correlate to increased expression of self-renewal and pluripotency pathways [66, 123]. Evidence suggests these cell surface proteins are not simply markers, but play an active role in CSC program.

Additional functional CSC markers have been identified in HNSCC. Activity of the detoxifying enzyme Aldehyde Dehydrogenase (ALDH) is elevated in HNSCC cell populations with increased tumorigenic, chemoresistant, and invasion and migration capabilities [124]. Similarly, high expression of ABC drug transporters is associated with oral cancer progression. Indeed, cells capable of dye efflux through ABC drug transporters, are considered HNSCC CSCs [125]. Elevated levels of epigenetic regulators, like BMI-1 of the polycomb repressive complex 1, have become associated with the CSC population and poor prognosis [126].

The pluripotency master regulators OCT4, SOX2, and NANOG have long been shown to be aberrantly active in HNSCC. All three factors are reactivated in HNSCC cell lines and oral cancer patients with the worst survival prognosis correlate with high OCT4 and NANOG expression [127, 128]. More recently, these transcription factors have been reported to play an active role in maintaining HNSCC CSC stemness. All three factors are upregulated in spheroid forming fractions of HNSCC [129]. Both OCT4 and SOX2 expression has been detected in primary oral cancer CSCs and are associated with early stage tumors [130, 131]. NANOG also displays increased expression in CSCs but interestingly is associated with late stage disease [132].

The discovery of CSCs has important implications for HNSCC patients. Markers such as CD44, ALDH activity, and pluripotency related factors may serve as important

prognostic tools or therapeutic targets. Evidence suggests that targeting HNSCC CSC populations could be effective in preventing metastasis and overcoming resistance [133].

1.4 Protein Turnover

Cellular protein levels are in a constant state of turnover. Continuous synthesis and degradation leads to steady state protein levels and cellular homeostasis [134]. Indeed, protein turnover plays an important role in regulating cellular fitness [135]. Concentrations, as well as spatio-temporal gradients, of proteins must be able to rapidly respond to both intra and extra-cellular cues and signals [136].

Protein turnover, or degradation, impacts a variety of basic cellular functions. Protein degradation works to recycle amino acids required for synthesis of new proteins and can generate active proteins through proteolytic cleavage or post translational modifications [137]. Another primary role of protein degradation is to serve as an intracellular quality control system through elimination of misfolded or damaged proteins. Accumulations of misfolded proteins can create non-physiological interactions with other proteins that are particularly harmful to the cell. Proteins are damaged in multiple ways, including genetic mutation, translational error, toxic factors from the environment, or intracellular toxic agents resulting from aging or disease. Damaged proteins must either be quickly repaired or eliminated in order to prevent further harm to the cell [138]. More recently, regulated protein degradation has been shown to control complex cellular processes including metabolism, cell cycle, transcription, signal transduction and apoptosis [135, 139].

Due to the amount of vital cellular functions influenced by protein turnover, it is not surprising that dysfunction in protein degradation has been implicated in multiple

diseases [134]. Aberrant protein stabilization or accelerated degradation of target proteins removes them from steady state levels, precipitating disease. Neurological diseases are the most intensively studied diseases related to dysfunction in protein turnover. In many cases, aggregates of disease specific proteins are unable to be degraded. In diseases such as Parkinson's disease, mutations in specific effector proteins have been identified and found linked to pathology [140, 141]. Other examples include Angelman syndrome and Liddle syndrome [142, 143]. Disruptions in protein turnover have also been identified in cancer, where stabilization of oncogenes and destabilization of tumor suppressors contribute to malignancy [144].

Proteins have developed specialized functions and are therefore degraded at widely different rates. The standard measurement is also known as protein half-life [145, 146]. Protein half-lives can range from just a few minutes to hours, in the case of transcription factors and regulatory proteins, to up to multiple days for structural proteins [138]. In order to control the various cellular functions regulated by protein turnover, cells must precisely control protein half-lives. The two predominant degradation systems in the cell responsible for regulating protein half-lives are autophagy and the Ubiquitin proteasome systems.

1.4.1 Autophagy

Derived from the Greek meaning "self-eating", autophagy is the process responsible for degradation of long-lived proteins, protein aggregates, and organelles. In typical cellular contexts, autophagy contributes to cellular homeostasis and quality control through protein degradation [147]. However, in times of cellular crisis, like nutrient starvation or oxidative stress, autophagy is increasingly activated as a protective

means [148]. Furthermore, dysregulation of autophagy has been shown to contribute to various disease states. Aside from its general role of protein degradation (macroautophagy), autophagy also encompasses sub-pathways involved in degradation of membrane bound cargo (microautophagy), mitochondria (mitophagy), and chaperone associated proteins [147].

Autophagy is a non-selective process that depends on the formation of a double membrane autophagosome [149]. Gradually formed out of a golgi like isolation membrane called the phagophore, the autophagosome engulfs a portion of the cytoplasm in order to take up its cargo [150]. Once its cargo is sequestered, the autophagosome fuses with lysosomes to form the autolysosome, where lysosomal acid proteases subsequently degrade its contents.

Key protein complexes involved in the initiation of autophagy include the ULK complex (ULK1/2), the mammalian ATG proteins (Atg12, LC3), and the class III phosphatidylinositol 3-kinase complex (Beclin-1) [151]. The kinase mTOR (mammalian target of rapamycin), when activated, is an upstream suppressor of autophagy. Negative regulation of the mTOR pathway by AMPK or p53 signaling promotes autophagy.

Inhibitors of critical steps in the autophagy pathway allow for experimental manipulation. For example, chloroquine is an agent that impairs lysosomal acidification while bafilomycin A1 is an antibiotic drug that inhibits autophagosome and lysosomal fusion [152]. Administration of either inhibitor in cell culture inhibits autophagy and will result in accumulation of autophagy specific proteins like LC3 and p62 [153]. If a protein of interest is also accumulated, it is likely degraded by autophagy.

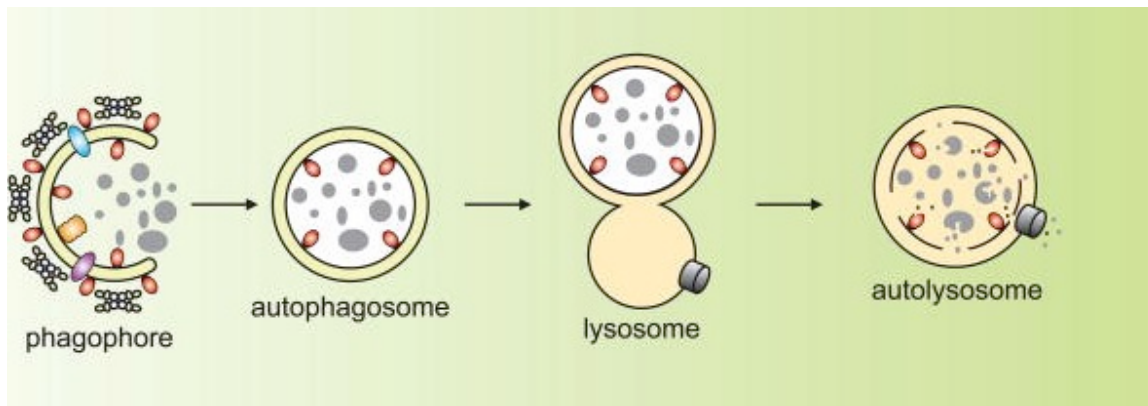


Figure 1.3 Schematic of Autophagy (Adapted from Yang, et al. *Curr Opin Cell Biol.* 2011)

1.4.2 The Ubiquitin Proteasome System

The Ubiquitin Proteasome System (UPS) is a highly regulated apparatus responsible for intracellular protein turnover and degradation [154, 155]. The UPS is a selective process orchestrated by a series of ubiquitin enzymes specific to the pathway. Generally, the UPS is responsible for degradation of proteins with shorter half-lives. However, the role of the UPS has been demonstrated in the turnover of up to 90% of all cellular proteins [156]. As the name Ubiquitin suggests, the UPS is involved in the regulation of a wide array of biological processes including antigen presentation, DNA repair, protein trafficking, epigenetic regulation, and cell cycle [154, 157].

The 26S proteasome is the large 2.5-MDa, ATP dependent multi-unit complex that catalyzes protein degradation in the UPS. The proteasome is composed of a 20S protein subunit, capped by two 19S regulatory subunits [158]. The proteolytic core, responsible for ATP dependent peptide-bond hydrolysis of substrate proteins, is contained in the barrel shaped 20S subunit. The 19S regulatory subunits recognize, de-ubiquitinate, unfold, and translocate proteins destined for degradation into the proteolytic core [159]. After proteasome processing, small 2-20 amino acid long peptides fragments remain, which are then reduced to single amino acids by nearby peptidases [160].

Proteasomes are present in high concentrations in the cell and are localized throughout the cytoplasm and nucleus [161]. The proteasome has become a drug target, as fluctuations in proteasomal activity and defects in function have been linked to a variety of diseases [162, 163]. Experimental methods used to ascertain half-lives of proteins degraded by the UPS also target the proteasome with inhibitors like MG132.

The ubiquitin gene encodes for a small, 76 amino acid protein weighing approximately 8.5 kDa. Ubiquitin is covalently conjugated to lysine residues of substrate proteins through an isopeptide linkage in a post translational process called ubiquitination [164]. Substrates include a variety of cellular proteins, including other ubiquitin molecules, which contain 7 lysine residues at Lys6, Lys11, Lys27, Lys29, Lys33, Lys48, and Lys63. Enzymatic linkage of ubiquitin molecules, also known as polyubiquitination, results in ubiquitin chains of varying length, structure, and function [165]. Examples include Lysine 48 ubiquitination, which targets proteins for degradation by the 26S proteasome, and Lysine 63 ubiquitination, which can activate transcription factors or function in protein scaffolding.

Ubiquitination occurs through an enzymatic cascade in three steps: activation, conjugation, and ligation. Each step is facilitated by a distinct ubiquitin enzyme. The initial step, activation of the ubiquitin molecule by an ATP dependent E1 ubiquitin enzyme, produces a ubiquitin-adenylate intermediate. Next, the activated ubiquitin is transferred to the active site of an E2 ubiquitin enzyme via a trans(thio)esterification reaction [166]. In the final ligation step, E3 ubiquitin enzymes facilitate the transfer, either directly (HECT domain E3s) or indirectly (RING domain E3s), of the ubiquitin molecule from the E2 enzyme to a lysine residue in the substrate protein. Successive

rounds of the ubiquitination process result in ubiquitin chains [167]. The specificity of ubiquitination increases with each step, as only two genes are responsible for E1 ubiquitin enzymes and only 35 genes for E2 enzymes. However, there are well over six hundred E3 ubiquitin ligases that recognize target substrate, thereby conferring specificity to the UPS [168].

E3 ubiquitin ligases fall into two main structural families that differ in how ubiquitin is transferred from E2 enzyme to substrate: the HECT (Homologous to the E6-AP Carboxyl Terminus) domain and the RING domain (Really Interesting New Gene) ligases [169]. HECT domain E3 ligases contain a catalytic cysteine residue that accepts the ubiquitin molecule from the E2 ligase, forming a thioester intermediate. It is the HECT domain E3 ligase that then directly transfers the ubiquitin to the substrate [170]. Approximately 30 HECT domain E3 ligases have been identified. Alternatively, ubiquitination with RING domain E3 ligases is facilitated by E2 ligases. The RING E3 ligase simply acts as a scaffold between the E2 ligase and substrate [171]. RING domain E3 ligases are the predominant family in mammals, with over 300 enzymes identified.

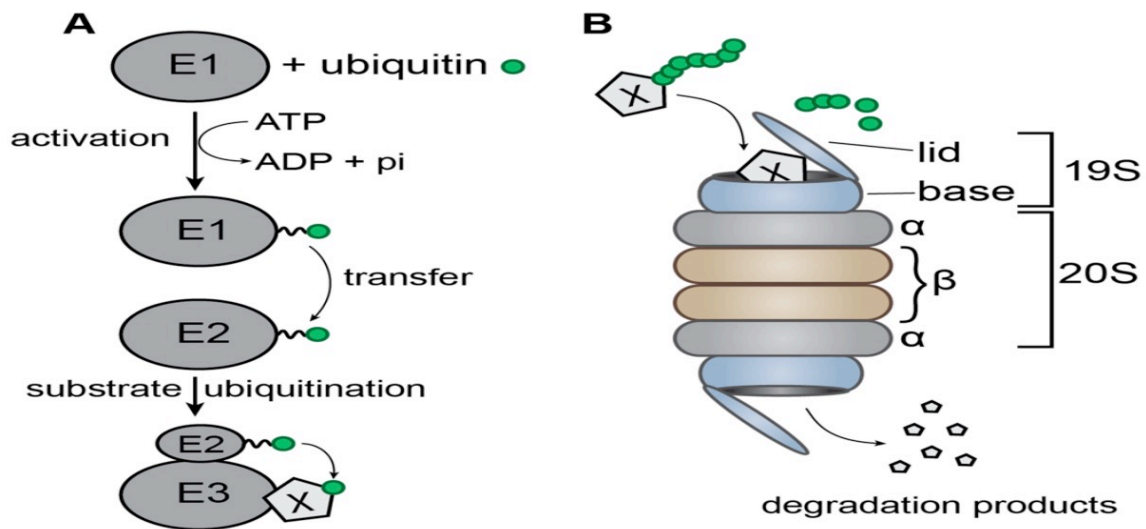


Figure 1.4 The Ubiquitin Proteasome System (Adapted from Seissler, et al. *Viruses*. 2017)

1.4.3 The E3 ubiquitin ligase RNF20

RNF20 (Ring Finger Protein 20) is a mammalian RING domain E3 ubiquitin ligase that shares homology with BRE1 of *S. cerevisiae*. RNF20, in complex with RNF40, is recognized as the main complex in monoubiquitination of the Lysine 120 residue of histone 2B (H2Bub1), a mark associated with actively transcribed genes. RNF20 regulates transcriptional elongation via its cooperative interaction with the FACT and PAF complexes [172]. In addition to transcription, RNF20 directed H2B monoubiquitination facilitates repair of DNA double strand breaks through homologous recombination, as well as mRNA end processing [173-175]. However, RNF20 E3 ubiquitin ligase activity is not limited to histone monoubiquitination, as it is also responsible for sending several proteins to the proteasome for degradation via Lysine 48 polyubiquitination [176, 177].

As with other histone modifying enzymes, RNF20 and H2B ubiquitination status play a critical role in the balance between stemness and differentiation. H2B de-ubiquitination has been reported essential for *Drosophila* stem cell maintenance [178]. RNF20 directed H2Bub1 is required for the differentiation of both embryonic and multipotent stem cells through activation of pro differentiation genes [179]. Further, increasing H2Bub1 marks actively induces differentiation of stem cells. USP22, the enzyme responsible for H2Bub1 de-ubiquitination, is downregulated during this differentiation process [180].

RNF20 is also involved in cancer, where it is suggested to play a role as a putative tumor suppressor [181]. Indeed, H2Bub1 levels are reduced in multiple cancers. Downregulation of RNF20 promotes increased malignancy through selective gene

expression in metastatic breast and parathyroid tumors [182, 183]. Interestingly, elevated expression of USP22 correlates with a cancer stem cell phenotype in lung cancer [184]. RNF20 directed polyubiquitination of target proteins also suppresses tumorigenesis through destabilization of cancer signaling pathways [176].

1.5 Scope of Work

Over the past two decades, the cancer stem cell hypothesis has become widely accepted by the cancer field. Due to its therapeutic implications, new treatment targets are continuously emerging. Of note, several developmental pathways and embryonic transcription programs have been reported as critical for CSC tumorigenesis, metastasis, and recurrence. The embryonic gene cluster ZSCAN4 has been found to play several critical roles in preimplantation embryonic development and pluripotent stem cells [1]. Recently, the Zalzman lab has demonstrated that ZSCAN4 is reactivated in multiple cancers, including HNSCC. However, a potential role of ZSCAN4 in cancer stem cells has not been demonstrated.

In this work, we have determined mechanisms that regulate protein turnover and important functions of ZSCAN4 in CSCs. We hypothesized that like other embryonic factors, ZSCAN4 plays a role in maintaining the CSC phenotype. We developed three types of HNSCC cell lines, with the appropriate isogenic controls, as tools to define the role of ZSCAN4 in cancer stemness. The first was a cell line expressing a reporter gene under the putative ZSCAN4 promoter that allowed us to monitor the cell populations expressing ZSCAN4. The second were ZSCAN4 knockdown cells lines, and the third allowed us to induce ZSCAN4 expression with the addition of tetracycline analog. We next utilized CSC specific biochemical assays to determine the effects of loss and

induction of ZSCAN4 on CSC properties both *in vitro* and *in vivo*. Chapter 2 presents our findings.

While ZSCAN4 expression is transient, little is known about its protein half-life or the mechanism(s) responsible for its turnover. Given the relevance of ZSCAN4 to mES cell and CSC physiology, we next sought to examine how ZSCAN4 protein levels are regulated. By controlling cellular translation, we determined the half-life of ZSCAN4 for the first time in human cells. Through inhibition of cellular degradation pathways, we found the mechanism responsible for ZSCAN4 degradation. Finally, ZSCAN4 co-immunoprecipitation and RNAi studies allowed us to identify and validate critical regulators of ZSCAN4 protein levels. Our data is presented in Chapter 3.

However, key questions have been raised during the process, and are addressed in Chapter 4, along with general conclusions and suggested future directions.

Chapter 2: ZSCAN4 promotes survival and growth of head and neck squamous cell carcinoma stem cells

2.1 Introduction

Cancers originating in the squamous cells that line the mucosal surfaces of the upper aerodigestive tract of the head and neck are classified as head and neck squamous cell carcinoma (HNSCC). HNSCC is a major public health concern, representing the sixth most prevalent malignancy globally [111]. Despite progress in current treatment options, HNSCC recurrence and metastasis overall has not significantly improved survival over the past few decades, particularly in patients presenting with advanced stage disease [121].

Recently, a subpopulation of cells within HNSCC tumors, termed Cancer Stem Cells (CSCs), has been identified. CSCs, also known as tumor initiating cells, have the ability to self-renew and efficiently elicit tumor formation [37, 66, 185-191]. These cells present similarities to stem cells and are suggested to be the driving force of tumorigenicity, contributing to an aggressive phenotype and tumor recurrence in multiple cancers [191, 192]. Additional properties of CSCs include the ability to form spheroids (tumorspheres) in non-adherent culture conditions [193] and resistance to genotoxic drugs. HNSCC CSCs also maintain high expression of the surface marker CD44 [37, 191, 194, 195], the polycomb repressive complex members EZH2 and BMI1 [37, 75, 196, 197] and the core pluripotency related genes expressed in embryonic stem (ES) cells such as OCT4, NANOG and SOX2 [66, 189, 198].

The Transcription factors OCT4, SOX2, and NANOG form a transcriptional network responsible for the maintenance of ES cell self-renewal and pluripotent differentiation potential [199]. Similarly, the early embryonic gene cluster *Zscan4* is essential for the

long term survival and preservation of developmental potency of mouse embryonic stem (mES) cells [1, 10]. ZSCAN4 promotes genomic stability in mES cells and has been shown to facilitate transcriptional reprogramming during the generation of induced pluripotent stem (iPS) cells through activation of early embryonic genes [1, 9, 15]. In combination with pluripotency transcription factors Oct4, Sox2, Klf4, and c-Myc, ZSCAN4 promotes a higher efficiency of nuclear reprogramming during generation of iPS cell lines ^[14]. ZSCAN4 is suggested to be involved in chromatin remodeling and epigenetic regulation. Indeed, ZSCAN4 expression corresponds to epigenetic changes such as histone H3 hyperacetylation, resulting in chromatin derepression that could contribute to early gene activation [1]. Much like other embryonic and pluripotent genes, the human ZSCAN4 has been proposed to have significance in cancer [16, 200]. However, to date, the function of ZSCAN4 in cancer has remained unknown.

Here we demonstrate ZSCAN4 as a novel cancer stemness factor. Our data indicate that ZSCAN4 is upregulated in head and neck squamous cell carcinoma (HNSCC) cell lines and is enriched in and marks the CSC population. We show that ZSCAN4 plays a critical role in promoting the CSC phenotype, as ZSCAN4 overexpression results in upregulation of CSC markers and the core pluripotency factors. Further, ZSCAN4 expression alters the chromatin landscape and gene expression to a profile more associated with embryonic stem cells, ultimately leading to a higher CSC frequency *in vitro* and *in vivo*. Conversely, loss of ZSCAN4 leads to downregulation of CSC markers and hypersensitivity to genotoxic drugs. Moreover, ZSCAN4 depletion results in reduced ability to form tumorspheres *in vitro* and significantly affects xenograft tumor growth *in vivo*. Overall, our studies indicate that ZSCAN4 is a critical factor for

the maintenance of HNSCC cancer stem cells, suggesting it is a novel target for future drug design and treatment of HNSCC.

2.2 Materials and Methods

Cell lines and cell culture. Head and neck squamous cell carcinoma (HNSCC) tumor cell lines TU167, TU159 and 012SCC were obtained from the University of Texas MD Anderson Cancer Center (Houston, TX, USA) [201]. The cells used in our laboratory were originally generated by Dr. Gary Clayman and were reported to be free of cross contamination (Zhao et al., 2011). The cell line 012SCC was donated by Bert O'Malley from the University of Pennsylvania School of Medicine (Philadelphia, PA, USA). All cell lines were tested free of mycoplasma. All tumor cell lines were cultured in complete DMEM medium (Invitrogen) supplemented with 10% fetal bovine serum (Atlanta Biologicals), 2 mM GlutaMAX (Gibco / ThermoFisher Scientific), penicillin (100 U/mL), streptomycin (100 µg/mL; Gibco / ThermoFisher Scientific).

Generation of ZSCAN4 knockdown and controls cells. Two HNSCC cells (Tu167, 012SCC) were transfected with 1 µg of pU6-ZSCAN4 shRNA vector (Origene) (containing RFP reporter and puromycin resistance gene), or controls: a non-targeting shRNA (NTC-shRNA) vector and an Empty vector (same plasmid without a shRNA cassette). Cells were transfected using Effectene reagent (QIAGEN) according to manufacturer's instructions. Cells were selected with 1 µg/ml Puromycin (ThermoFisher Scientific). Knockdown was confirmed by immunostaining and by qPCR.

Quantitative reverse transcriptase polymerase chain reaction (qRT-PCR). RNA was isolated with Trizol and 1 µg of total RNA was reverse transcribed by Superscript III (Invitrogen) following the manufacturer's protocol. For qPCR, 10 ng cDNA was used per well in triplicates using SYBR green (Roche) following the manufacturer's protocol. Reactions were run on the LightCycler 480 system (Roche). Fold induction was calculated by the delta delta Ct method. A standard curve was made for reference gene by serial dilutions of genomic DNA from 100 ng to 3.125 ng. The following primers were used: ZSCAN4 forward 5'-ATCCACCTGCCTTAGTCCAC-3' and ZSCAN4 reverse 5'-TCGAAGAAGTGTCCAGCCA-3', RPLP0 forward 5'-CAGCAAGTGGGAAGGTGTAATCC-3' and RPLP0 reverse 5'-CCCATTCTATCATCAACGGGTACAA-3', OCT4 forward 5'-TCTTCAGGAGATATGCAAAGC-3' and OCT4 reverse 5'-ATCCTCTCGTTGTGCATAGT-3', SOX2 forward 5'-CAAGGAGAGGCTTCTTGCTGA-3' and SOX2 reverse 5'-CACAGAGATGGTTCGCCAGT-3', and NANOG forward 5'-AGCTACAAA CAGGTGAAGAC-3' and NANOG reverse 5'-TAGGAAGAGTAAAGGCTGGG-3'.

Immunohistochemistry. Cells were fixed in 4% PFA for 10 min at room temperature. Cells were permeabilized with 0.2% NP-40 for 10 min. Cells were then blocked for 10 min at room temperature in 1% BSA, 10% fetal bovine serum, and 0.2% Tween 20 and incubated overnight at 4°C with the primary antibodies in a blocking solution: a Primary antibodies (ThermoFisher Scientific) were incubated over night at the following dilutions: mouse anti-ZSCAN4 (1:1000), mouse anti-NANOG (1:400), mouse anti-OCT4 (1:400), and mouse anti-SOX2 (1:100). Slides were incubated for 1 hour at room temperature with secondary antibodies (Thermofisher Scientific; diluted in block

solution): Alexa 488 Donkey anti Rabbit (1:400); Alexa568 Donkey anti mouse (1:800). Nuclei were stained with DAPI (Roche Life Sciences) for 10 min at room temperature. Scramble non-targeting (NTC) shRNA cells and empty vector cells were used as positive controls. Additional controls were cells stained without primary antibody. Cells were visualized under a Zeiss 510-confocal microscope.

Generation of pZSCAN4-mCherry cells

The region containing the ZSCAN4 promoter (2.5Kb upstream of transcription start codon, and downstream 299 base pairs downstream) has been cloned into a lentiviral vector (pEZX- LvPM02). In this plasmid, the mCherry reporter gene and a puromycin resistance gene have also been inserted downstream of the putative ZSCAN4 promoter. One-way ANOVA of our qPCR results indicates a correlation between high mCherry and ZSCAN4 expression ($F_{(2)}=28.62$; $p<0.0005$). A Tukey's posthoc comparison suggests that both negative (Neg) and low positive (Low-Pos) mCherry expressing cells have lower ZSCAN4 levels compared to high positive (High-Pos) mCherry expressing cells ($p's<0.01$), validating a direct correlation between mCherry and ZSCAN4 expression.

Immunoblot

To detect endogenous ZSCAN4 in Tu167 cells, cells were harvested by accutase (Millipore). Cytoskeleton buffer (10 mM PIPES, 300 mM sucrose, 100 mM NaCl, 3 mM $MgCl_2$, 1 mM EGTA and 0.5% Triton X100) was used to fractionate cytosolic proteins. To isolate nuclear lamina fractions, pellets were then lysed in urea solution (8 M Urea in 0.01 Tris pH 8 + 0.1 M NaH_2PO_4) and sonicated. Equal amounts of protein were electrophoresed on 10% polyacrylamide gels and transferred to a PVDF membrane. Membranes were blocked

with 5% nonfat milk for 1 hour, incubated with the indicated primary antibodies for 2 hours at room temperature, rinsed, and then incubated with secondary antibody (1:5000) for 1 hour. Secondary antibodies were visualized by ECL chemiluminescence (ThermoFisher Scientific).

Antibody	Company	Dilution
ZSCAN4	Origene	1:1k
OCT4	BD Transduction Labs	1:1k
SOX2	Abcam	1:1k
NANOG	Abcam	1:1k
BMI-1	Abcam	1:1k
EZH2	BD Transduction Labs	1:1k
H3K27ac	Cell Signaling	1:1k
H3K56ac	Cell Signaling	1:1k
H3K14ac	Cell Signaling	1:1k
H3K18ac	Cell Signaling	1:1k
H3K9ac	Cell Signaling	1:1k
H3	Cell Signaling	1:1k

Table 2.1 List of Antibody Dilutions.

Tumorsphere Formation Assay

Monolayer cells were cultured in complete DMEM medium (Invitrogen) supplemented with 10% fetal bovine serum (Atlanta Biologicals), 2 mM GlutaMAX (Invitrogen), penicillin/streptomycin (50 U / 50 ug/ml; Invitrogen). Cells were harvested using accutase (EMD Millipore), collected by centrifugation (500 RPM, 5 min), and replated at density of 50,000 cells per well in 6 well ultra-low attachment dishes. The tumorsphere growth was performed in DMEM F12 (Invitrogen), supplemented with 2% B27 serum replacement (Invitrogen), 200 ng basic FGF (Affymetrix, eBioscience), 200 ng recombinant human EGF (Biolegend), and 100 mg/ml Ampicillin (American Bioanalytical). Tumorspheres were maintained in culture for the duration of 11 days. Size and number of spheres were analyzed using ImageJ software.

Drug Treatment Assay

Cells were cultured in 2 cm² wells of 24 well plates (15,000 cells per well) for 24 hours. Cells were treated in triplicate at multiple concentrations (0 ng-1600 ng) of Mitomycin C (Sigma), Cisplatin (Sigma), or Bleomycin (Sigma). Cells were incubated in MMC: 8 hours, CPT: 24 hours or BLM: 3 days. Following treatment, cells were washed twice with PBS and allowed to incubate in fresh drug free culture medium for 72 additional hours. Wells were then incubated in 2.5 mg/ml MTT (Sigma) for 2 hours followed by incubation with DMSO. Optical density (O.D) absorbance was measured on a plate reader at 570 nm.

***In vivo* tumor growth**

The *in vivo* experimental protocol conformed to the guidelines of the Institutional Animal

Care and Use Committee of University of Maryland, School of Medicine (protocol # 0714014). Twenty three immune compromised NSG (NOD/SCID/IL2R γ ^{-/-}) [202] female mice (Charles River), at 2 months of age, were subcutaneously injected into the flank with 1×10^6 ZSCAN4 knockdown, non-targeting control (NTC) shRNA, or WT Tu167 cells.

Data analysis

Data were analyzed with individual t-tests, one-way ANOVAs, or two-way ANOVAs with repeated measure, as specified in figure legends. Significant interactions were followed by Tukey or Bonferroni post-hoc comparisons when appropriate. STATSTICA 13 and GraphPad Prism 5 softwares were used for data analyses and formation of the figures.

2.3 Results

2.3.1 ZSCAN4 is highly expressed in a fraction of HNSCC cells

In order to determine the expression of ZSCAN4 in HNSCC, we first screened a panel of HNSCC cell lines (012SCC, SCC13, Tu167, Tu159) for ZSCAN4 by quantitative reverse transcription PCR (qRT-PCR; **Fig 2.1A**) and immunoblot analysis (**Fig 2.1B**). Our data indicate ZSCAN4 is expressed in HNSCC cells, while normal human tissue controls are negative.

Prior studies in mES cells have shown that m*Zscan4* is transiently expressed in a small fraction of cells in culture at a given time. However, with time ZSCAN4 expression is gradually activated in all cells [200]. To study ZSCAN4 expression in HNSCC and to enrich for ZSCAN4 expressing cells, a plasmid containing the mCherry reporter gene

under the ZSCAN4 promoter (pZSCAN4-mCherry) was used to generate a lentiviral vector. Two separate HNSCC lines (Tu167 and 012SCC) were stably transduced to generate pZSCAN4-mCherry cells (**Fig. 2.1C**). We then sorted the cells by fluorescence activated cell sorting (FACS) to collect mCherry negative cells and compared them to low and high mCherry expressing cells. Our real time qRT-PCR analysis of ZSCAN4 in the sorted cells validates a positive correlation between mCherry and ZSCAN4 expression levels (**Fig. 2.1D**). Our data indicate that the frequency of ZSCAN4 expression in cancer is similar to that in mES cells, as approximately $2.77\pm 0.44\%$ of the 012SCC cells and $0.7\pm 0.03\%$ of the Tu167 cells were mCherry positive (**Fig 2.1E**).

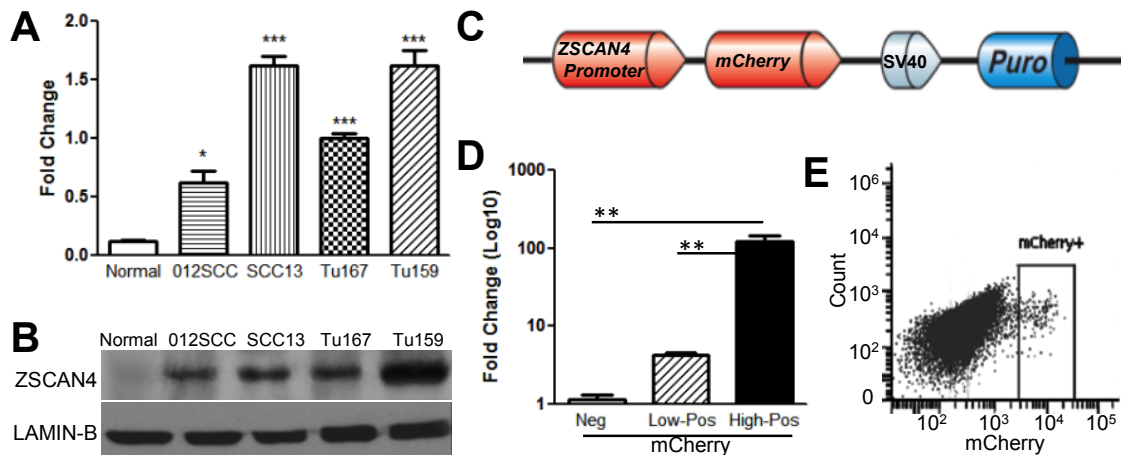


Figure 2.1 Expression of ZSCAN4 is upregulated in Human head and neck cancers **A**, ZSCAN4 is upregulated in HNSCC cell lines, as shown by qPCR and by **B**. Immunoblot analysis, whereas normal human tonsil primary cell lines and normal human tonsil tissue controls from different donors are negative. Error bars indicate S.E.M. **C**, A schematic illustration of mCherry reporter under the ZSCAN4 promoter Lenti viral vector. **D**, ZSCAN4 expression correlates with mCherry expression as demonstrated by real-time RT-qPCR assay. All data shown as mean±S.E.M. observed in triplicate in at least three independent experiments. Asterisks indicate a significant difference from normal cells (a.) or from Neg (d.): * $p < 0.05$, ** $p < 0.01$, *** $p < 0.001$. **E**, FACS sorting of pZSCAN4-mCherry positive and negative cells

2.3.2 ZSCAN4 marks tumorsphere forming cells in HNSCC

Cancer Stem Cells represent a rare portion of the tumor population [195]. Due to their capacity for self-renewal, CSCs can be experimentally enriched for by their ability to form spheroids (tumorspheres) in non-adherent culture conditions [188, 203]. Upon tumorsphere formation, we found that $0.6\% \pm 0.06$ of our Wild type (WT) Tu167 cells and $0.81 \pm 0.12\%$ of our 012SCC cells possess tumorsphere-forming ability (**Fig. 2.2A**). After 8 days of tumorsphere formation, cells were collected to define ZSCAN4 protein levels by immunoblot. We found that ZSCAN4 is elevated in tumorspheres compared to monolayer controls (**Fig. 2.2B**).

Next, to determine if ZSCAN4 activity contributes to tumorsphere formation, we used our pZSCAN4-mCherry cells (Tu167) to select for mCherry/ZSCAN4 positive cells by FACS sorting and performed a tumorsphere formation assay. Our data indicate that enrichment of the culture with high mCherry/ZSCAN4 positive cells leads to significantly enhanced ability to form tumorspheres when compared to WT cells ($p < 0.01$) and mCherry negative control cells ($p < 0.01$) (**Fig. 2.2C-E**). Positive mCherry expression also correlates positively with spheroid size (**Fig. 2.2D**). Consistent with the upregulation of ZSCAN4 observed during tumorsphere formation, we noted that some negatively sorted cells were able to reactivate mCherry in the tumorsphere conditions (**Fig. 2E**). These findings suggest that ZSCAN4 expression is enriched for within the tumorsphere population and correlates with an enhanced ability to form tumorspheres.

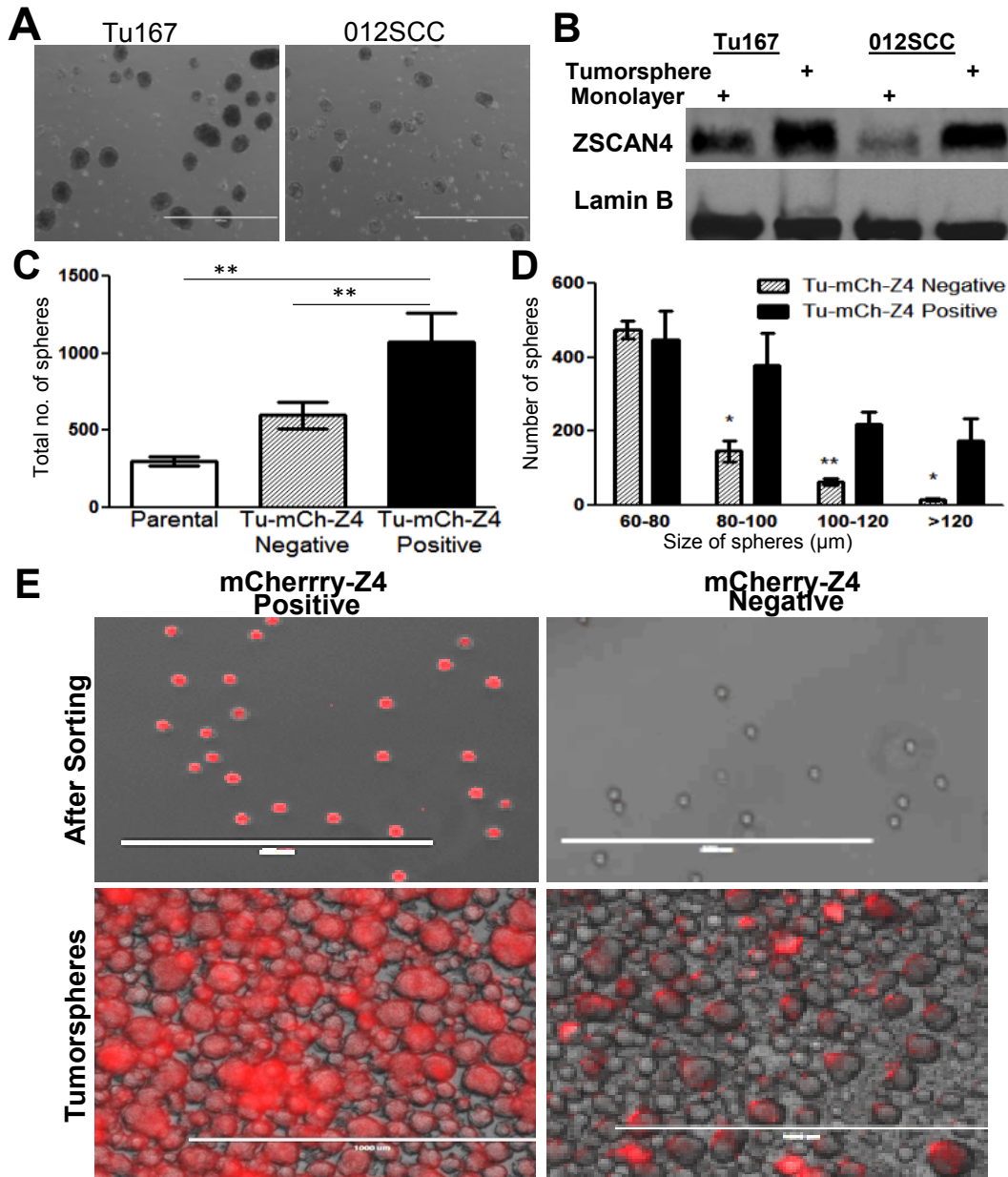


Figure 2.2 ZSCAN4 marks cancer stem cells in HNSCC **A**, Representative image of tumorspheres in WT HNSCC cell lines Tu167 and 012SCC. **B**, Immunoblot analyses indicate that ZSCAN4 expression is enriched for in tumorspheres. **C**, Tumorsphere formation assay show a total increase in the number of tumorspheres in mCherry/ZSCAN4 (Tu-mCherry) positive cells compared to tumorspheres from mCherry negative and tumorspheres generated from WT cells (parental). **D**, Classification of tumorspheres according to size demonstrate a major increase in the larger tumorspheres. **E**, Representative images showing ZSCAN4 expression marks cells with higher ability to form tumorspheres as FACS sorting for mCherry (mCh) positive and negative and subsequent tumorsphere formation leads to significant increase in the number and size of tumorspheres when compared to mCherry negative cells. All data shown as mean \pm S.E.M. observed in triplicate in at least three independent experiments. Asterisks indicate a significant difference from Tu-mCherry-Positive cells: * p <0.05, ** p <0.01.

2.3.3 ZSCAN4 expression promotes the CSC phenotype

CSCs harness pluripotency mechanisms to improve survival and have been reported to display higher expression levels of OCT4, NANOG, KLF4 and SOX2 [66, 84, 188-191]. These core pluripotency factors have been shown to not only to mark CSCs, but to promote CSC survival and self-renewal [19, 66, 204, 205]. Furthermore, these factors are associated with higher grade HNSCC tumors and poorer clinical survival [19, 204]. Importantly, ZSCAN4 has previously been found to activate early embryonic genes in mES cells [10, 206]. Therefore, we next sought to study the effects of ZSCAN4 expression on CSC markers. To that end, we developed a lentiviral vector in which ZSCAN4 expression is triggered by addition of doxycycline (Dox), a tetracycline analog, to the culture medium. Our vector also included an rTTA fused to GFP and a puromycin selection gene. We then generated Dox inducible ZSCAN4 HNSCC cell lines (Tu167) that we named thereafter tet-ZSCAN4. A short induction of ZSCAN4 by incubation with Dox for 48 hours resulted in upregulation of ZSCAN4 expression (in Tu167 cells). Our data by qRT-PCR show that ZSCAN4 induction leads to significant upregulation of OCT4 ($p < 0.01$), NANOG ($p < 0.0001$), KLF4 ($p < 0.01$) and SOX2 ($p < 0.01$) (**Fig. 2.3A**). Our results were further validated in another HNSCC cell line (012SCC) (**Fig. 2.3B**). ZSCAN4 induction also increased the expression of the CSC surface marker CD44, as indicated by immunostaining (**Fig. 2.3C**). These data indicate ZSCAN4 expression leads to an upregulation of CSC markers, including pluripotent stem cell factors.

2.3.4 ZSCAN4 induction facilitates chromatin remodeling

To accommodate the transcriptional programs that maintain pluripotency, ES and iPS cells adopt an open chromatin state [207]. Indeed, for efficient iPS cell generation,

transcriptional reprogramming and reacquisition of an open chromatin state is required [208]. Interestingly, murine *Zscan4* expression has been found to correlate with more efficient nuclear reprogramming during generation of iPS cells, as well as with heterochromatin decondensation marks in mES cells, specifically through histone hyperacetylation [14, 209]. To determine if expression of human ZSCAN4 leads to similar epigenetic changes in cancer cells, we examined acetylation patterns on Histone 3 Lysine residues 9, 14, 18, 27, and 56 (H3K9ac, H3K14ac, H3K18ac, H3K27ac, H3K56ac) after ZSCAN4 induction. We show by immunoblot analysis that acetylated histone marks are significantly elevated, particularly on Lysine residues 14, 18, 27 and 56 (**Fig. 2.3D**). These data suggest ZSCAN4 induction leads to a global H3 hyperacetylation. Therefore, to explore further functional relations between ZSCAN4, its effect of H3 hyperacetylation and gene expression we performed multiple chromatin immunoprecipitation (ChIP) assays with antibodies specific to H3K27ac, H3K14ac. We used as a negative control the antibody for H3K9ac, as our immunoblot data showed this histone acetylation mark remained at comparable levels after ZSCAN4 induction. As our results indicated that ZSCAN4 significantly affects NANOG expression, we chose to examine its promoter region using ChIP-qPCR. Interestingly, while chromatin mark H3K9ac was not enriched at the NANOG promoter, H3K27ac and H3K14ac were significantly enriched for after ZSCAN4 induction (**Fig. 2.3E**). Our data suggest that induction of ZSCAN4 leads to functional hyperacetylation at NANOG promoter, suggesting its role in chromatin decondensation and promoting CSC factor expression and phenotype.

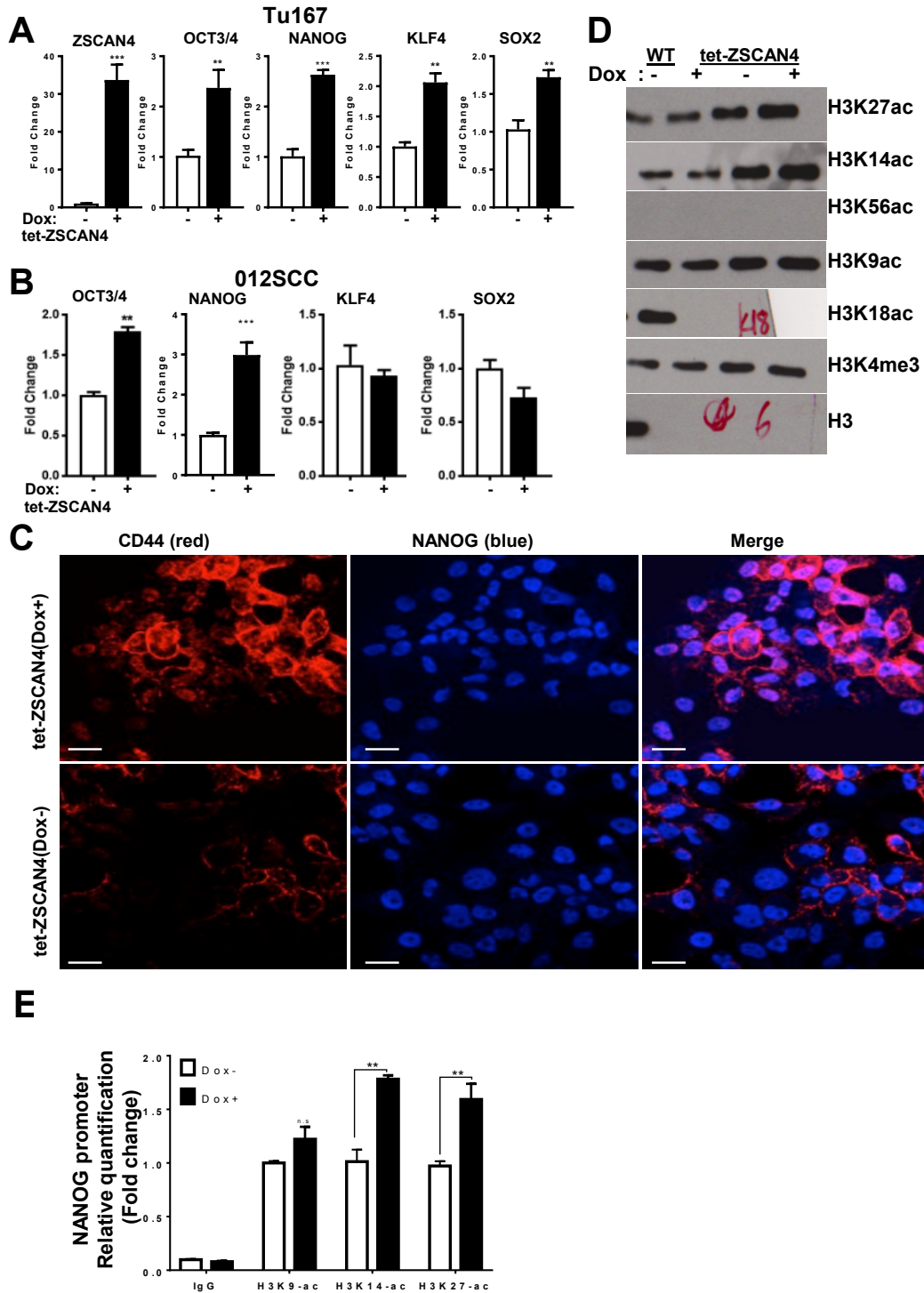


Figure 2.3 Induction of ZSCAN4 promotes the cancer stem cell phenotype. ZSCAN4 induction results in a significant increase in **A,B**, pluripotency factors expression (*OCT4*, *NANOG*, *KLF4*, and *SOX2*) in HNSCC cell lines **C**, frequency of cells presenting the CSC marker CD44 and **D**, histone acetylation marks. **E**, Enrichment of histone acetylations at the NANOG promoter after ZSCAN4 induction. Data shown as mean±S.E.M. *** Asterisks indicate $p < 0.001$.

2.3.5 ZSCAN4 induction increases tumorsphere formation ability *in vitro* and the frequency of CSC derived tumors *in vivo*

Along with an increase in CSC markers, our data indicate that ZSCAN4 induction increases both the number and size of tumorspheres *in vitro* as shown by a tumorsphere formation assay (**Fig. 2.4A, B**). In order to determine whether the observed increase in tumorsphere number and size is accompanied by an increased frequency of CSCs, we employed extreme limiting dilution assays (ELDA). HNSCC tet-ZSCAN4 cells (Tu167 and 012SCC) were treated, or kept untreated, for 48 hours in Dox to induce the expression of ZSCAN4. Next, cells were harvested, serially double diluted at concentrations starting from 1,000 cells per well to less than 1 cell per well and then grown in non-adherent tumorsphere-promoting culture conditions. Tumorspheres were counted after 5 days in culture per each dilution, and CSC frequency was calculated using ELDA software [210]. Our results indicate a significant, 3 fold increase ($p < 0.003$) in the frequency of tumorsphere initiating cells following ZSCAN4 induction for 48 hours prior to tumorsphere formation (**Fig. 2.4C**).

CSCs are ultimately defined by their ability to form tumors upon injection at extremely low cell numbers into immune-deficient mice. To validate our data, and determine the frequency of CSCs, we utilized the ELDA *in vivo* assay in the immune compromised NSG (NOD/SCID/IL2R γ ^{-/-}) mouse xenograft model [202]. tet-ZSCAN4 (Tu167) cells were treated or untreated with Dox for 48 hours in culture and then injected into the right and left flanks of NSG mice at concentrations ranging from 100 to 100,000 cells and monitored over 60 days (**Fig. 2.5A**). No Dox was given to the mice throughout the experiment. Remarkably, our data indicate that ZSCAN4 induction dramatically increases the frequency of CSCs. We found that injection of 100,000 cells in both condition formed tumors after approximately 20 days. However, ZSCAN4 induction led

to measurable tumors at dilution of 10,000 cells per injection more rapidly than untreated cells. Further, extreme dilution to 1,000 cells show that ZSCAN4 induced cells have the ability to form tumors, while the untreated cells at the same concentrations formed no tumors for the duration of the experiment for 60 days (**Fig. 2.5B,C**). Our results by ELDA software show that ZSCAN4 induction prior to inoculation increases CSC frequency by approximately 6 fold (**Fig. 2.5D**). Overall, our data show that ZSCAN4 induction significantly increases CSC frequency both *in vitro* and *in vivo* and further suggests a predominant role for ZSCAN4 in the promotion of the CSC phenotype.

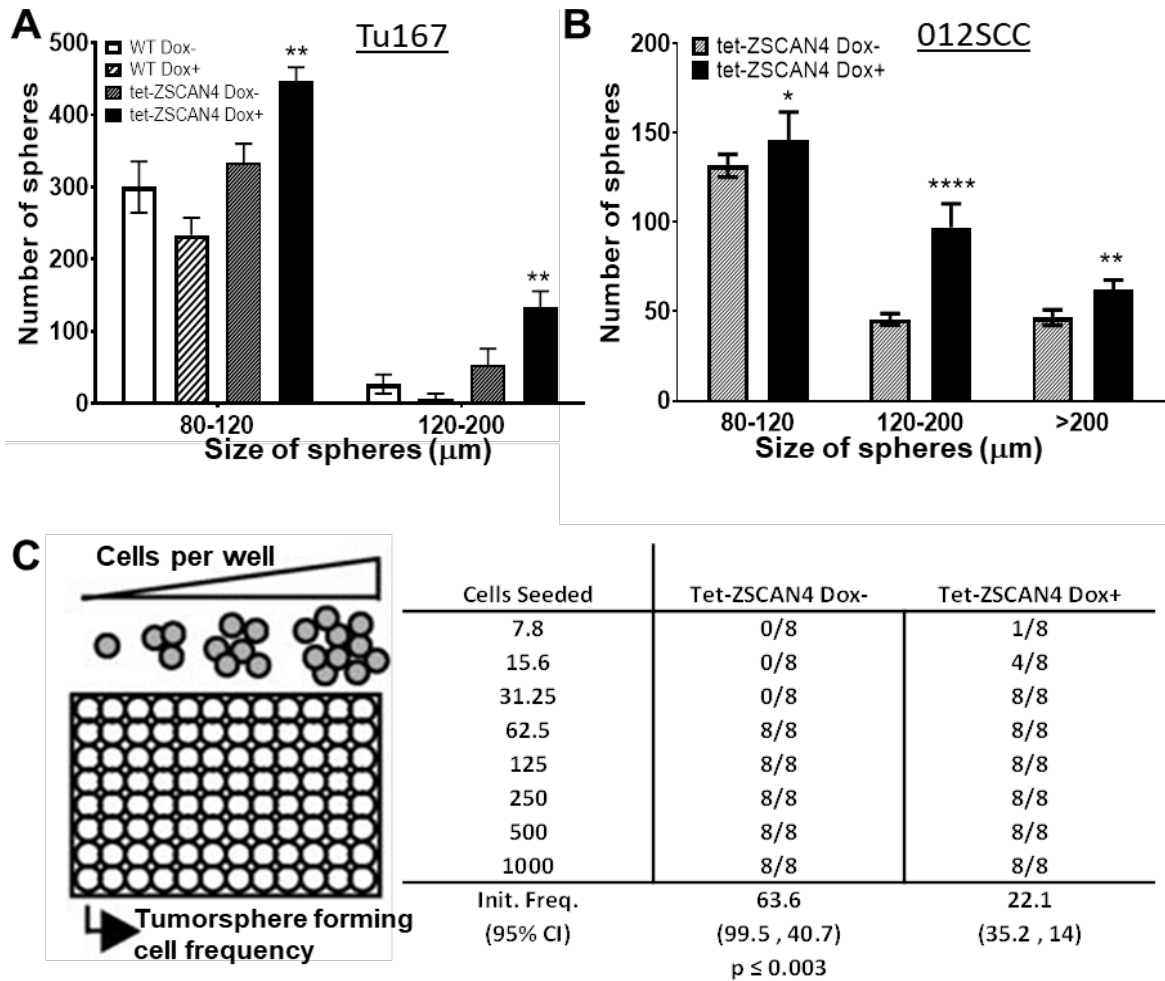


Fig. 2.4. ZSCAN4 increases tumorsphere formation. **A.** Induction of ZSCAN4 by addition of Dox for 48 hours (Dox+), prior to generation of tumorspheres, in tet-ZSCAN4 Tu167 cells or **B.** 012SCC cells, significantly increases the number and size of tumorspheres compared to untreated isogenic controls (Dox-) and to wild type (WT) Dox±. Asterisks indicate a significant difference from isogenic untreated and WT cells: ** $p < 0.01$, *** $p < 0.001$, **** $p < 0.0001$. **C.** Illustration of *in vitro* extreme limiting dilution assay (ELDA) and results show that ZSCAN4 induction prior to tumorsphere formation assay significantly increases the frequency of CSC; $p < 0.003$.

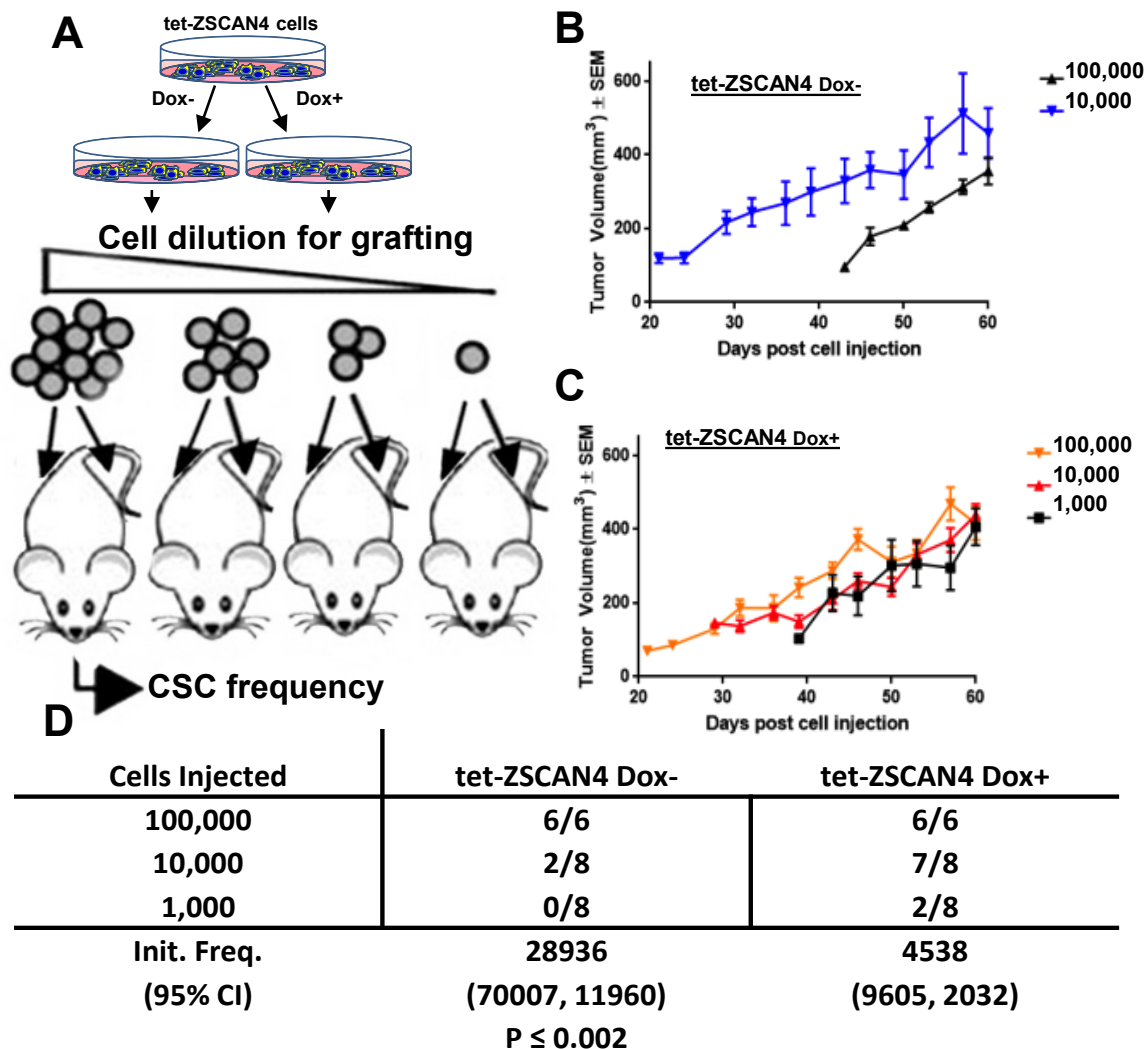


Fig. 2.5. ZSCAN4 increases CSC frequency and tumor formation. **A** ELDA *in vivo*: An illustration of mouse xenograft ELDA to study CSC frequency by extreme limiting dilution assay. **B-D**. To perform *in vivo* ELDA, tet-ZSCAN4 (Tu167) cells treated or untreated with Dox, were injected subcutaneously into the right and left flank of NOD/SCID gamma immunodeficient mice in multiple increased dilution: 100,000 cells, 10,000 cells, 1000 cells and 100 cells per inoculation (n=8 tumors), in NSG mice and allowed to form tumors for up to 31 days.

2.3.6 ZSCAN4 is required for maintenance of the CSC phenotype and tumorsphere formation

We next sought to determine the effect of ZSCAN4 depletion on cancer stem cell marker expression. Our results by qPCR and immunoblot assay show that ZSCAN4 depletion in HNSCC results in downregulation of the same pluripotency factors that are upregulated after ZSCAN4 induction (**Fig. 2.6A,B**). Next, we examined additional CSC markers EZH2 and BMI1. EZH2 has been shown to be enriched in a variety of cancer type CSC subpopulations, including HNSCC where it is required for CSC survival [76, 211]. BMI-1 is upregulated in multiple cancers where it promotes the CSC phenotype and its expression correlates with poor prognosis [75, 196, 197]. Consistent with the reduction in the core pluripotency markers, our results indicate significant decreases in BMI1 and EZH2 (**Fig. 2.6B**). These data suggest that depletion of ZSCAN4 alters HNSCC CSC potency.

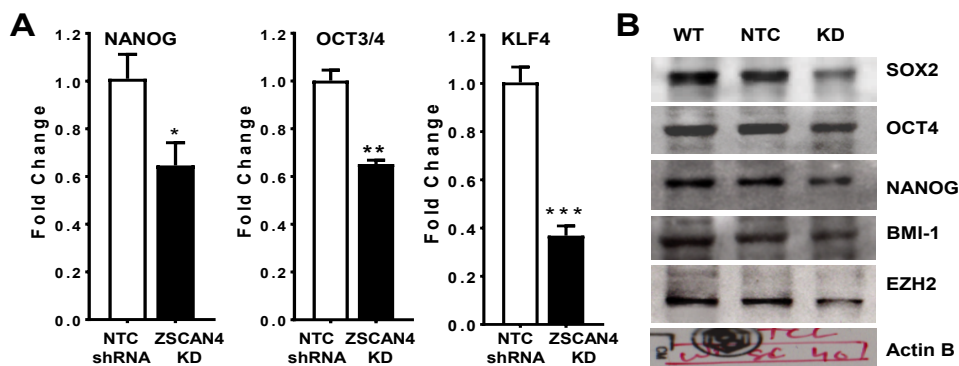
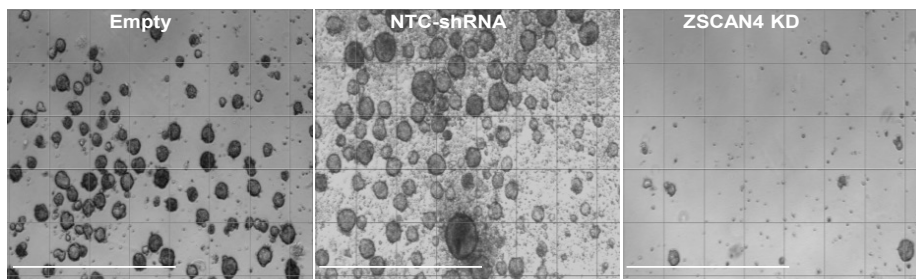


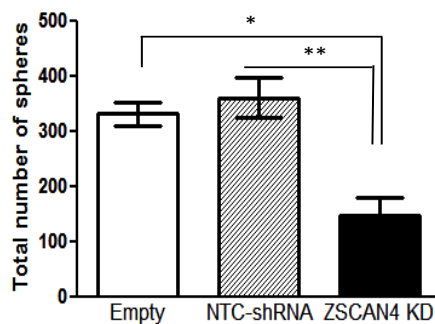
Figure 2.6. ZSCAN4 is required for the expression of cancer stem cell markers **A**, Real-time RT-qPCR analysis of ZSCAN4 knockdown (KD) in Tu167 and 012SCC indicate that loss of ZSCAN4 results in decrease expression of the pluripotent stem cell factors NANOG, OCT3/4, and KLF4 compared to non-targeting control (NTC) shRNA in isogenic HNSCC control cells. Asterisks indicate: * $p < 0.05$, ** $p < 0.01$, *** $p < 0.001$ (t-test). **B**, Immunoblot analysis validate the reduction in pluripotency and CSC factors after ZSCAN4 knockdown. Compared to wild type (WT) and isogenic cells expressing NTC-shRNA expressing normal levels of ZSCAN4.

To determine if ZSCAN4 is necessary for tumorsphere formation and survival of cancer stem cells, we performed tumorsphere formation assays in ZSCAN4 knockdown cell lines and isogenic NTC-shRNA control cells. Our results indicate that ZSCAN4 depletion leads to a dramatic reduction in both overall tumorsphere number and size (**Fig. 2.7A-C**) ($p<0.01$). Further, ZSCAN4 knockdown leads to reduced ability to form large spheres compared to both NTC-shRNA and Empty vector cells controls (**Fig. 2.7C**) ($p<0.0001$). Our data suggest that the source of these effects lies in a reduced self-renewal capacity to form spheres following ZSCAN4 depletion. Collectively, our data indicate that ZSCAN4 is essential for the survival and self-renewal of HNSCC CSCs.

A



B



C

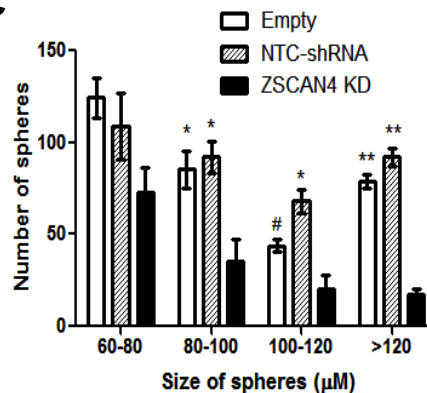


Figure 2.7 ZSCAN4 is essential for tumorsphere growth and survival **A**, Representative images of tumorspheres in ZSCAN4 control vs depleted cells. **B**, ZSCAN4 Knockdown (KD) results in fewer and **C**, smaller tumorspheres when compared to both control cell lines (Empty and NTC-shRNA). All data shown as mean±S.E.M. observed in triplicate in at least three independent experiments. Asterisks indicate: * $p<0.05$, ** $p<0.01$, # $p=0.07$

2.3.7 ZSCAN4 depletion leads to hypersensitivity to genotoxic drugs

Another hallmark of CSCs is multi-drug resistance, a major factor contributing to cancer recurrence (reviewed in [212]). Therefore, we examined the role of ZSCAN4 in response to genotoxic drugs. To define the effect of ZSCAN4 on drug resistance, we measured cell viability after increasing doses of the DNA damaging drugs in ZSCAN4 depleted and control Tu167 cells. Drugs tested include Cisplatin (CPT), one of the major DNA crosslinking chemotherapeutic drugs used to treat HNSCC, Mitomycin C (MMC), another DNA crosslinker, and Bleomycin (BLM), a radiomimetic agent. As shown in **(Fig 2.8 A,B)**, treatment of ZSCAN4 depleted cells with the crosslinking drugs MMC and CPT results in significantly decreased cell viability compared to isogenic control NTC shRNA cells. Treatment of ZSCAN4 depleted Tu167 cells with BLM, a radiomimetic drug that simulates the DNA damage caused by radiation treatment, resulted in dramatically reduced cell viability compared to NTC-shRNA isogenic controls **(Fig. 2.8C)**. These effects were confirmed by three separate two-way ANOVAs with repeated measure of drug exposure providing significant cell line by drug exposure interaction (MMC: $F_{(3)}=5.46$, $p<0.05$; CPT: $F_{(3)}=9.8$, $p<0.01$; BLM: $F_{(3)}=85.7$, $p<0.0001$). Bonferroni posthoc tests for each drug verified significant reduction in cell viability following ZSCAN4 depletion for each of the comparisons (all p 's <0.05). Altogether, our data indicate that ZSCAN4 depletion leads to hypersensitivity to genotoxic drugs, further implicating ZSCAN4 as a functional marker for CSCs.

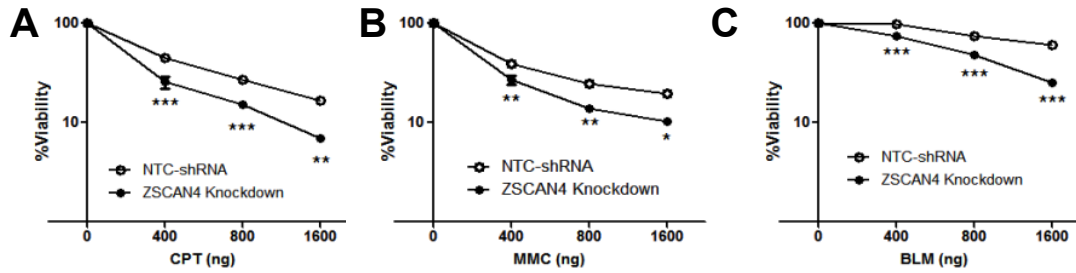


Figure 2.8 ZSCAN4 Depletion leads to hypersensitivity to genotoxic drugs. ZSCAN4 depleted cells display hypersensitivity to genotoxic drugs when compared to non-template control (NTC) shRNA. Increasing doses of **A**, Cisplatin (CPT), **B**, Mitomycin C (MMC), and **C**, Bleomycin (BLM) and their viability was measured by MTT assay. All data shown as mean±S.E.M. observed in triplicate in at least three independent experiments. Asterisks indicate: * $p<0.05$, ** $p<0.01$, *** $p<0.001$.

2.3.8 ZSCAN4 depletion severely affects tumor growth

CSCs maintain an enhanced ability to form tumors [29, 192]. We therefore next studied the impact of ZSCAN4 depletion on tumor formation *in vivo* using the immune compromised NSG mouse as a xenograft model. We subcutaneously injected either 1×10^6 ZSCAN4 knockdown, non-targeting control (NTC) shRNA, or WT Tu167 cells into the flanks of female NSG mice (**Fig. 2.9A**). Our data indicate that ZSCAN4 depletion leads to a drastic tumor growth inhibition (**Fig. 2.9B**). WT and NTC shRNA control cells display robust tumor formation within two weeks while knockdown cells take approximately three weeks to reach a palpable size. After 32 days of growth, control tumors reach an average size of 450mm^3 while ZSCAN4 knockdown tumors present an 89% growth inhibition in tumor size. This observation was supported by a two-way ANOVA with repeated measures analysis ($F_{(2,4)}=6.25$; $p<0.0001$). A Bonferroni posthoc test verified a significant difference in tumor volume between ZSCAN4 knockdown treated group and the two control groups (NTC-shRNA: Days 20-31 and WT: Days 24-31). Overall, our results suggest that ZSCAN4 depletion severely affects tumor growth *in vivo*.

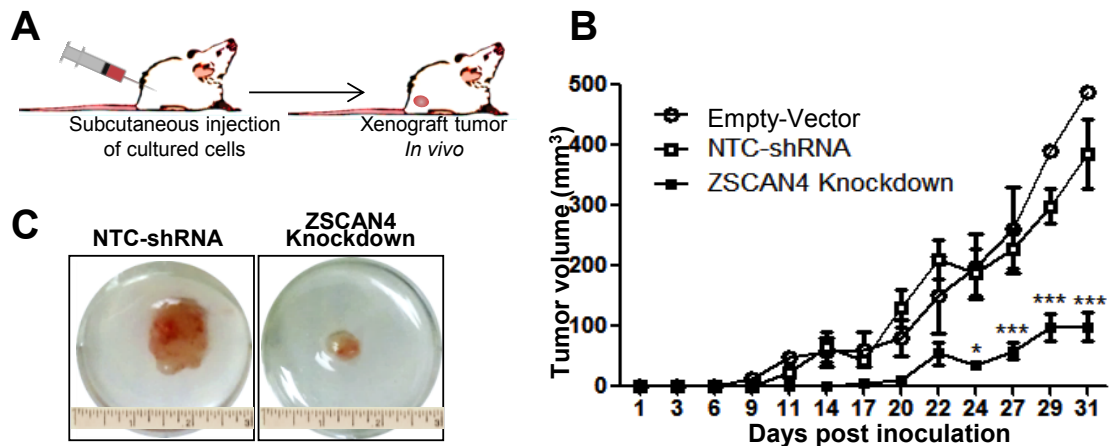


Figure 2.9 ZSCAN4 depletion severely affects tumor growth
A, An illustration of mouse xenograft cancer tumor model. Cells were injected subcutaneously with either ZSCAN4 Knockdown (n=10), or NTC-shRNA as controls (n=10) in NGS mice and allowed to form tumors for up to 31 days. **B**, Mean±SEM of tumor volume (mm³) as measured at indicated days following injection. Asterisks represent a significant difference between ZSCAN4 Knockdown and the other groups at the marked days: * $p < 0.05$, *** $p < 0.001$. ZSCAN4 Knockdown cells were significantly smaller starting from day 14 and continuously. **C**, Representative pictures of NTC-shRNA and ZSCAN4 depleted tumors in 30 mm plates, harvested at the termination of the experiment.

2.4 Discussion

HNSCC remains a growing public health issue as its incidence is expected to continue to rise worldwide [111]. Advances in single modality treatments of early stage malignancy have improved some patient outcomes. Surgical and localized radiotherapeutic innovations have led to improved tissue functionality and upgraded reconstructive surgical procedures reduce defects caused by invasive surgeries [119]. However, late stage HNSCC, constituting over 60% of all diagnosed HNSCC cases, remains difficult to treat [110, 120]. For locally advanced and metastatic HNSCC, multi-modal treatment involving combinations of surgery, radiotherapy, and chemotherapy have become the standard of care [110]. Unfortunately, these therapies have not

significantly improved survival, with treatment failure attributed to local tumor recurrence and metastasis [213]. Therefore, new therapeutic approaches are needed.

Recent studies have reported a population of CSCs within HNSCC tumors [214]. Here we demonstrate for the first time the critical role of ZSCAN4 in the maintenance and promotion of HNSCC CSCs. We show that ZSCAN4 is highly expressed in HNSCC cell lines and is limited to a small percentage of the total HNSCC population, much like the CSC population. After selecting for ZSCAN4 positive cells, we observed both an increase ability to form tumorspheres *in vitro* and a significant increase in CSC frequency and tumor formation *in vivo*. Further, we observed higher levels of ZSCAN4 after enrichment of the CSC population through tumorsphere formation assay. Altogether, these findings suggest that high levels of ZSCAN4 mark the HNSCC CSC population.

Our findings suggest that ZSCAN4 not only marks CSCs, but that ZSCAN4 facilitates the CSC phenotype. Prior studies detail the function of ZSCAN4 in the maintenance of pluripotent stem cells such as mES and iPS cells through activation of early embryonic genes. Like ZSCAN4, embryonic factors OCT4, SOX2, and NANOG are reactivated in cancer and have further been classified as CSC markers that regulate self-renewal and contribute to tumor aggressiveness and metastasis. We demonstrate that upon induction of ZSCAN4 in HNSCC, CSC markers including CD44 and embryonic factors OCT4, SOX2, NANOG and KLF4 are upregulated.

Similar to findings in mES cells, ZSCAN4 expression led to a derepressed chromatin state marked by histone hyperacetylation [209]. We found that a short induction of ZSCAN4 leads to a global change in chromatin state as acetylation marks increased on Lysine residues 9, 14, 18, 27, and 56 of Histone 3. We further found that

hyperacetylation was localized to the NANOG promoter. As in mES cells, open chromatin in CSCs may contribute to maintenance of potency through activation of embryonic transcription networks or could contribute to a more rapid DNA damage response to genotoxic therapeutics [209, 215].

The ZSCAN4 induced CSC phenotype was also demonstrated by functional assays. *In vitro*, ZSCAN4 induced cells increased the CSC frequency, as determined by spheroid formation and ELDA. Remarkably, *in vivo*, ZSCAN4 induction increased CSC frequency over 6 fold. These results demonstrate that ZSCAN4 increases the number of CSCs in culture, leading to more robust tumors initiation *in vivo*.

Importantly, we demonstrate that ZSCAN4 maintains the CSC phenotype. Loss of ZSCAN4 by gene knockdown leads to a decrease in CSC markers including pluripotency factors and polycomb repressive complex genes. Moreover, upon the loss of ZSCAN4, tumorsphere size and overall number was significantly reduced. Consistent with these findings, ZSCAN4 knockdown leads to hypersensitivity to DNA damaging drugs currently used in the clinic. Increased sensitivity to Mitomycin C, Cisplatin, and Bleomycin after knockdown indicates a role for ZSCAN4 in drug resistance, another CSC trait.

Remarkably and consistently, ZSCAN4 knockdown results in dramatically reduced tumor formation ability *in vivo*. We observed an 89% growth inhibition in knockdown tumors compared to control tumors, indicating that anti-ZSCAN4 treatment could be effective on its own. Additional studies will be required to determine the combined effects of genotoxic drugs and targeted ZSCAN4 inhibition *in vivo*.

Our findings that ZSCAN4 marks, promotes, and maintains the most highly tumorigenic population of cells suggest that it may serve as a unique target for eradicating the most resistant cancer cells that underlie recurrence following HNSCC treatment. While the current acceptable treatment for HNSCC following surgery consists of radiation therapy or cisplatin treatment, our data suggests additional targeted inhibition of ZSCAN4 could function synergistically to enhance its efficacy.

Chapter 3: ZSCAN4 is negatively regulated by the ubiquitin-proteasome system and the E3 ubiquitin ligase RNF20

3.1 Introduction

The embryonic gene *Zscan4* (Zinc finger and SCAN domain containing 4) promotes telomere and genomic stability in mouse embryonic stem (ES) cells [200]. Knockdown of *Zscan4* in mouse ES cells results in telomere shortening and karyotype abnormalities, slowing cell proliferation until reaching culture crisis. *Zscan4* is highly but transiently expressed [200], with protein expression bursts that facilitate chromatin remodeling [9, 10] and transcriptional reprogramming during the generation of induced pluripotent stem (iPS) cells [14, 15, 216]. A short expression burst of *Zscan4* was further demonstrated to replace *Myc* and enhance the efficiency of mouse iPS cell formation through activation of early embryonic genes [15]. The human ZSCAN4 has been shown to interact with factors important for telomere maintenance [16, 217], and has been suggested to play a role in cancer [16, 200]. Given the important role of ZSCAN4 and its transitory nature in the cell [2, 200], maintaining the delicate balance between its protein synthesis and degradation is critical for stem cell and potentially cancer cell function.

Concentrations and spatial gradients of specific proteins must be able to rapidly change in response to extracellular cues and according to current cell state [136]. Small protein imbalances can drastically impact such important cellular processes. Therefore, intracellular protein degradation and turnover play an important role in cell life cycle [135]. Two major pathways responsible for the degradation of proteins in cells are

autophagy and the ubiquitin proteasome system (UPS). Autophagy is the process responsible for degradation of longer lived, structural proteins and organelles. This process depends on the formation of a double membrane autophagosome, which takes up its cargo and subsequently fuses with lysosomes, leading to degradation [147, 150]. The canonical UPS is an ATP-dependent degradation pathway [156]. Proteins are marked for proteasomal degradation by ubiquitin, a small 8.5 kDa regulatory protein, which is added to lysine residues of the target protein. Polyubiquitination, or formation of a ubiquitin side chain, specifically on lysine residue 48 of the ubiquitin moieties, targets proteins to the 26S proteasome for degradation. The ubiquitination process involves three steps: activation of the ubiquitin molecule by E1 ubiquitin enzymes, conjugation of ubiquitin to an E2 ubiquitin ligase, and ligation of the ubiquitin molecule to substrate. E3 ubiquitin ligases play a particularly important role as they connote substrate specificity and facilitate the ligation of the ubiquitin molecule to the target protein [164].

Transient expression of high levels of *Zscan4* [200] leads to acquisition of stem cell properties and potency [9, 10]. Therefore, stringent regulation of the ZSCAN4 protein is required to effectively control its cellular functions. However, the regulation of human ZSCAN4 protein, and more specifically its turnover dynamics, remains obscure. As a growing body of evidence suggests a vital role for ZSCAN4 in stem cells and cancer, knowledge of its protein regulation is critical. In this study, we demonstrate for the first time that ZSCAN4 protein degradation is regulated by the ubiquitin-proteasome system. Further, we identify the E3 ubiquitin ligase RNF20 as an important negative regulator of ZSCAN4 protein stability.

3.2 Materials and Methods

Cell Culture

Tu167 cells were obtained from the University of Texas MD Anderson Cancer Center (Houston, TX, USA). All cell lines used in this study were grown in complete DMEM medium (Invitrogen) supplemented with 10% fetal bovine serum (Sigma), 2 mM GlutaMAX, penicillin (100 U/mL), streptomycin (100 µg/mL) and were tested free of mycoplasma.

RNF20 knockdown by siRNA

Wild type (WT) Tu167 cells were grown in monolayer to 70% confluence and transfected with 25 nM of either ON-TARGETplus individual siRNAs (targeting sequences GCUAAACAGUGGAGAUAAU and GUAUCAUCCUAAAACGUUA) or SMARTpool siRNA reagent targeting human RNF20 (Dharmacon). For non-targeting control conditions, Tu167 cells were transfected with 25 nM MISSION siRNA Fluorescent Universal Negative Control siRNA (Sigma,). Cells were transfected using DharmaFECT reagent (Dharmacon) according to manufacturer's instructions. Knockdown was confirmed after 48h incubation by immunoblot.

Determination of ZSCAN4 half-life

WT and doxycycline (Dox) inducible tet-ZSCAN4 Tu167 cells were treated with 1µg/mL Dox (or kept untreated) for 24h to induce ZSCAN4. For RNF20 knockdown, WT Tu167 cells were transfected for 48h with either NTC-siRNA, pool RNF20 siRNA or RNF20 siRNA1-2 as described above. Cells were treated with 25 µg/ml CHX (Sigma), for the

indicated time points. Total cell lysate in RIPA buffer was loaded on 10% SDS PAGE gel and immunoblotted with ZSCAN4 antibodies (1:1000; Origene;) or controls, β -actin (1:1000; Millipore) and Lamin B antibodies (1:2000; Santa Cruz). Band intensities of ZSCAN4 were quantified using ImageJ software [218] and normalized to controls. The relative levels of ZSCAN4 in sample not treated with CHX was considered as initial level of ZSCAN4 and considered as 1 unit. The half-life of ZSCAN4 was determined using formula $t_{1/2} = \ln 2/k$ (k is the slope of the degradation curve).

Autophagy Pathway Assay

tet-ZSCAN4 Tu167 cells were treated for 24h with Dox and then autophagy inhibitors: 5nM of Bafilomycin A1 or 25 μ M of Chloroquine (Sigma) were added for 24h. Whole cell lysate (50 μ g) in RIPA buffer was used on 8 % SDS-PAGE analyzed by immunoblot to visualize the following antigens: anti-ZSCAN4 (1:1000; Origene), anti-p62 (1:5000; Sigma), anti-LC3 (1:1000; CellSignaling Technology), Anti-Beta Actin (1:10,000; Millipore). All data shown represent at least 3 independent experiments.

Immunoblot Analysis

Nuclear proteins were fractionated using Nuclear Extraction Kit following manufacture's protocol (Active Motif). Total cell lysate was prepared in RIPA buffer and sonicated. For the detection of endogenous ZSCAN4 in Tu167 cells, cells were harvested by accutase (Millipore) and Cytoskeleton buffer (10 mM PIPES, 300 mM sucrose, 100 mM NaCl, 3 mM $MgCl_2$, 1 mM EGTA and 0.5% Triton X100) was used to fractionate cytosolic proteins. Then, pellets were lysed in urea solution (8 M Urea in 0.01 Tris pH 8 + 0.1 M NaH_2PO_4) and sonicated. Nuclear proteins were electrophoresed in 8% polyacrylamide

gels and transferred to a PVDF membrane. Immunoblot was performed using the following primary antibodies: ZSCAN4 (Origene;1:1000), GAPDH (Santa Cruz; 1:5000), Actin (Sigma; 1:500), Lamin B (Santa Cruz; 1:2000) and with HRP (horseradish peroxidase) conjugated secondary antibodies (Millipore; 1:5000). Protein bands were detected using Pierce ECL Western Blotting Substrate (Thermo Scientific). SuperSignal West Femto (Thermo Scientific) was used to detect endogenous ZSCAN4 in Tu167 cells. All immunoblots shown represent at least 3 independent experiments.

Ubiquitination Assay

WT Tu167 cells were treated with indicated concentration of MG132 for 3-12h. Cells treated with vehicle only were used as controls. Nuclear protein was isolated using urea extraction buffer. Then, 100 µg of nuclear lysate was diluted in IP-RIPA buffer with 0.1% SDS and denatured by heating to 90° C for 10 minutes. Samples were taken for co-immunoprecipitation and immunoblot analyses.

Co-Immunoprecipitation

WT Tu167 were lysed in RIPA buffer and sonicated. Protein A/G beads (Invitrogen) were incubated with 1 µg of anti-ZSCAN4 in 100 µL of RIPA buffer without SDS for 1h at room temperature. Then, the beads were washed twice with RIPA buffer and crosslinked to the beads with 5 mM BS3 solution (ThermoFisher Scientific) according to manufacturer's protocols. Then the beads were pre-cleared with 100 µg of nuclear lysate in 100 µl IP buffer without SDS (Cell Signaling Technology) overnight at 4°C. Cell lysates were loaded and bound antigens were eluted with 25 µL RIPA with 0.1% SDS

and 25 μ L of 2x loading dye. Proteins were separated in 10% SDS PAGE and immunoblotted with corresponding antibodies.

Immunofluorescence Confocal Microscopy

Cells were fixed in ice cold methanol/acetic acid (3:1). The fixed cells were dropped on microscope slides. Antigen retrieval was performed followed by blocking for 10 min at room temperature. Primary antibody was incubated overnight at 4°C for the following antigens: ZSCAN4 (Origene, 1:1000), RNF20 (Cell Signaling, 1:2000), and Ubiquitin Lysine 48 (Millipore 1: 2000). The slides were washed and incubated with secondary antibodies conjugated with Alexa-488 or 568 at room temperature for 1h and then treated with DAPI and To-Pro-3 to stain the nuclei. Slides were mounted and visualized by a Zeiss 510-confocal microscope. Co-localization analyses were performed by ImageJ software [218].

Quantitative reverse transcriptase polymerase chain reaction (qRT-PCR). RNA was isolated by Trizol (Life Technologies) and 1 μ g of total RNA was reverse transcribed by Superscript III (Invitrogen) following the manufacturer's protocol. Then, 10 ng cDNA was used per well in triplicates using SYBR green (Roche) following the manufacturer's protocol. Real time PCR was performed on LightCycler 480 (Roche). Fold induction was calculated by the absolute quantification method. Primers used: ZSCAN4 forward 5'-ATCCACCTGCCTTAGTCCAC-3' and ZSCAN4 reverse 5'-TCGAAGAAGTGTCCAGCCA-3', and RPLP0 reverse 5'-CCCATTCTATCATCAACGGGTACAA-3'.

Statistical analyses. All data and representative images shown are the result of at least three independent experiments, with biological replicates. Student's t-test, one-way or two-way ANOVAs with repeated measures were followed by Tukey's posthoc comparison tests (when appropriate) for statistical analyses. Statistical analyses were performed with STATISTICA-12 and GraphPad-Prism7 software. All P values <0.05 were considered as statistically significant.

3.3 Results

3.3.1 ZSCAN4 protein turnover and half-life

Zscan4 expression is transient and limited to a small fraction of cells, suggesting it requires tight regulation at the protein level. Interestingly, ZSCAN4 has been found to be relatively stable in mouse ES cells, with a half-life of up to 6h [12]. While normal physiological expression is limited to early stage embryonic cells, ZSCAN4 has been shown to be aberrantly reactivated in cancer [16]. Therefore, we chose to study ZSCAN4 protein stability in the human head and neck cancer cell line Tu167. To determine ZSCAN4 half-life, Tu167 cells were incubated with the protein translation inhibitor cycloheximide (CHX) and ZSCAN4 concentration was monitored by immunoblot over 10h. The CHX chase assay indicates that ZSCAN4 protein half-life is 8.3h (**Fig. 3.1A, B**).

ZSCAN4 is weakly expressed in the human cell line Tu167. Therefore, in order to further study ZSCAN4 in these cells, we developed a doxycycline (Dox) inducible ZSCAN4 lentiviral vector. We used this vector to generate inducible ZSCAN4 cells (Tu167) and named them tet-ZSCAN4. Addition of Dox, a tetracycline analog, to the

media results in ZSCAN4 induction. Our immunoblot analysis reveals that ZSCAN4 is induced in these cells as early as 12h (**Fig. 3.1C**) and as expected, is localized to the nucleus (**Fig. 3.1D**). Using our tet-ZSCAN4 cell line, we then analyzed the stability of the ZSCAN4 protein. Cells were treated for 24h with Dox and then incubated with CHX. ZSCAN4 concentration was again monitored by immunoblot over 10h. Our CHX chase assay indicates that the induced ectopic ZSCAN4 protein half-life of 8.0h is similar to the endogenous ZSCAN4, suggesting its utility as a tool to further study ZSCAN4 stability (**Fig. 3.1E, F**). These data together suggest that the stability of the human ZSCAN4 in human cancer cells is similar to that of mouse ES cells [12].

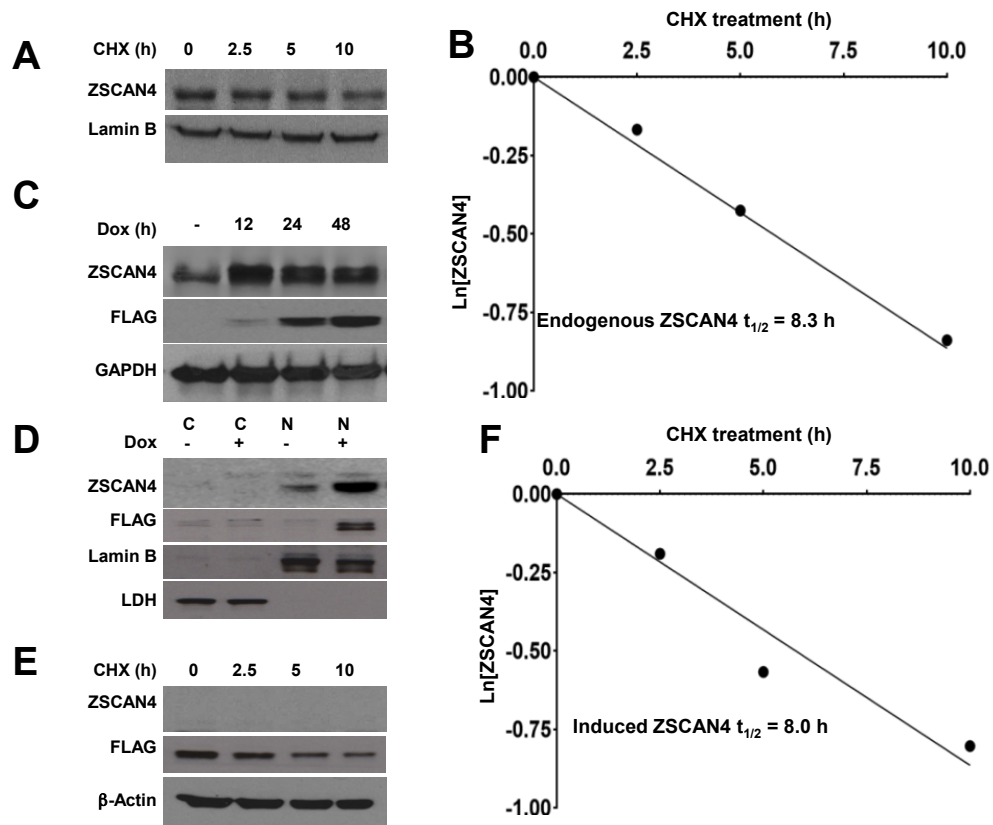


Figure 3.1 Human ZSCAN4 protein half-life and cellular localization. **A.** Immunoblot analysis of ZSCAN4 in wild type Tu167 cells after treatment with the translational inhibitor cycloheximide (CHX) results in decreased ZSCAN4 protein concentration. **B.** Protein half-life analysis indicates that endogenous ZSCAN4 protein half-life is 8.3h. **C.** Immunoblot analyses show addition of Dox to medium for 0-48h (Dox (h)) results in higher expression of ZSCAN4, and ZSCAN4-FLAG is induced as early as 12h. **D.** Fractionation of the cells content to cytoplasmic (C) and nuclear (N) proteins, show the endogenous ZSCAN4 (anti-ZSCAN4) as well as the FLAG-tagged ectopic ZSCAN4 (anti-FLAG), are localized to the nucleus. **E.** Isogenic Doxycycline (Dox) induced tet-ZSCAN4 cells after treatment with CHX by immunoblot and **F.** protein half-life analysis indicate that the ectopic ZSCAN4 protein half-life is 8.0h. Images and results represent data of at least three independent experiments.

3.3.2 ZSCAN4 degradation is proteasome dependent

We next sought to determine the pathway responsible for ZSCAN4 turnover and degradation. We first examined the possible clearance of ZSCAN4 by autophagy. tet-ZSCAN4 cells (Tu167) were incubated for 12h with autophagy inhibitors Bafilomycin A1 and Chloroquine [150]. Our immunoblot analysis shows that both p62 and LC-3, two proteins specifically degraded by autophagy, accumulate in the cells (**Fig 3.2A**). These results indicate that the autophagy pathway was successfully inhibited. However, ZSCAN4 levels remained unchanged (**Fig 3.2A**), excluding autophagy as the mechanism responsible for ZSCAN4 turnover.

This prompted us to examine the UPS. We incubated tet-ZSCAN4 cells with the proteasome inhibitor MG132 at multiple time points. Our data indicate a time dependent accumulation of ZSCAN4 through the 12h incubation (**Fig 3.2B**). Furthermore, we show a time dependence (**Fig 3.2C**) and a dose response (**Fig 3.2D**) to proteasome inhibition by MG132. These data show that UPS inhibition results in ZSCAN4 accumulation and suggests it is the pathway by which ZSCAN4 protein is degraded.

To exclude that the response was specific to the exogenous ZSCAN4 induction, we treated wild type (WT) Tu167 cells with 5uM MG132 for 0-12h. Our results validate that endogenous ZSCAN4 accumulates with proteasome inhibition (**Fig 3.2E**). These data indicate that both the endogenous and the induced ZSCAN4 proteins are not degraded by autophagy but instead in a proteasome dependent manner.

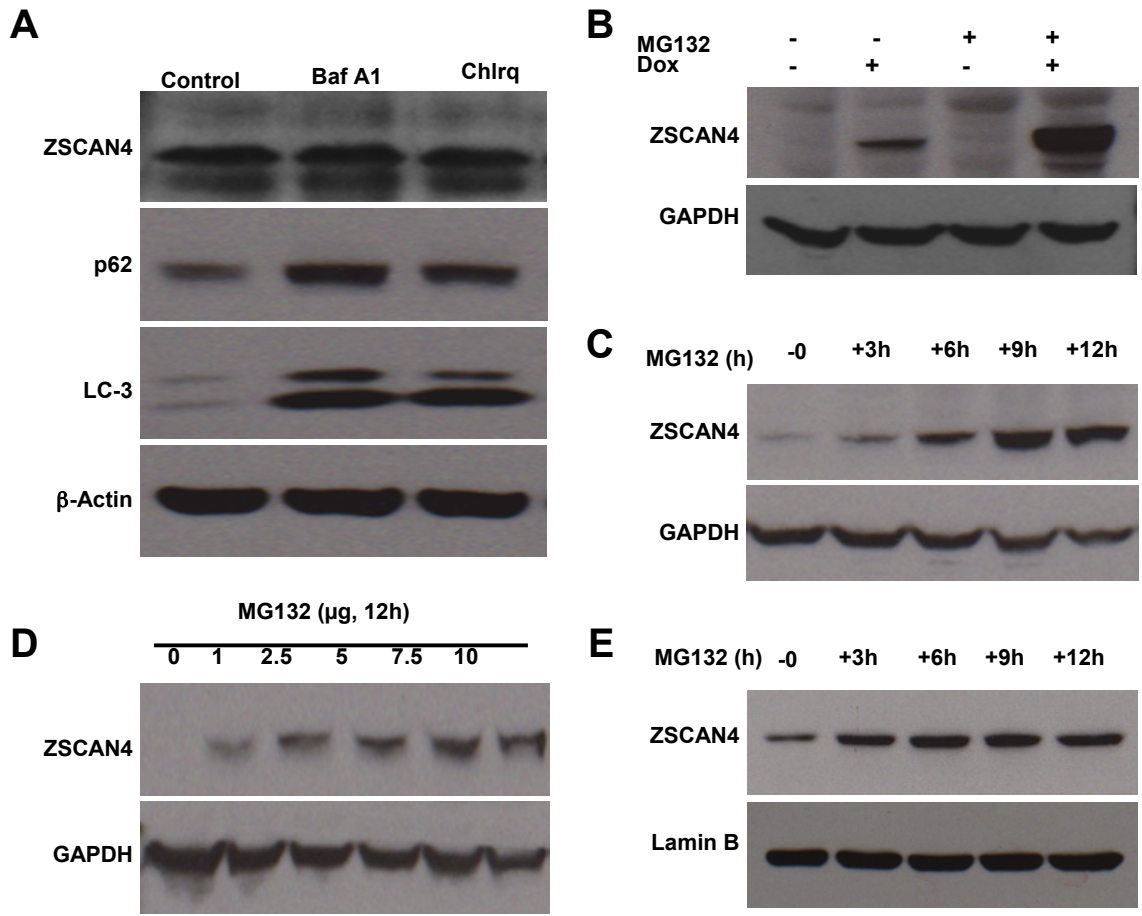


Figure 3.2 ZSCAN4 degradation is proteasome dependent **A.** Immunoblot analyses indicate that inhibition of autophagy with Bafilomycin A1 and Chloroquine results in accumulation of autophagy targets p62 and LC-3. However, ZSCAN4 was not affected. **B.** Overexpression of ZSCAN4 by Dox followed by inhibition of the proteasome with the proteasomal inhibitor MG132 demonstrates ZSCAN4 accumulates in the cells. **C-D.** Kinetics experiments show that accumulation of ZSCAN4 following proteasome inhibition by MG132 occurs in a time and dose dependent manner. **E.** Similar studies performed in wild type (WT) cells show the accumulation of the endogenous ZSCAN4 with the treatment of proteasome inhibitor MG132 suggesting this pathway is significant for the regulation of ZSCAN4 protein.

3.3.3 ZSCAN4 is marked for proteasomal degradation by lysine 48 ubiquitination

Protein turnover allows for clearance of non-functional proteins. Proteins destined for degradation by the proteasome are tagged by ubiquitin side chains [219]. Lysine 48 ubiquitin side chains, also known as K48 polyubiquitination, connote specificity to proteasomal degradation [164]. Therefore, we next examined if ZSCAN4 is lysine 48 polyubiquitinated by inhibiting the proteasome with MG132 for 12h in WT Tu167 cells. Then, we selected for covalently bound K48 ubiquitin chains by performing ZSCAN4 IP experiments in denaturing conditions. Following ZSCAN4 IP, we immunoblotted with a lysine 48 ubiquitin (K48-Ub) antibody and observed a strong ubiquitin signal at the 50 kDa molecular weight of ZSCAN4 (**Fig 3.3A**). Moreover, a large smear above the 50 kDa band indicates ZSCAN4 with bound ubiquitin side chains of varying lengths (**Fig 3.3B**).

To further validate the lysine 48 polyubiquitination of ZSCAN4 protein, WT Tu167 cells were treated with or without MG132 for 5h and co-immunostained for anti-K48-Ub and anti-ZSCAN4 (**Fig 3.3C**). Co-localization analysis indicates that about 5% of ZSCAN4 co-localizes with K48-Ub in the untreated conditions, whereas this fraction is 4 fold higher following 5h inhibition of the proteasome with MG132 (**Fig 3.3D, E**). Our data suggest that ZSCAN4 is targeted to the proteasome via canonical lysine 48 polyubiquitination.

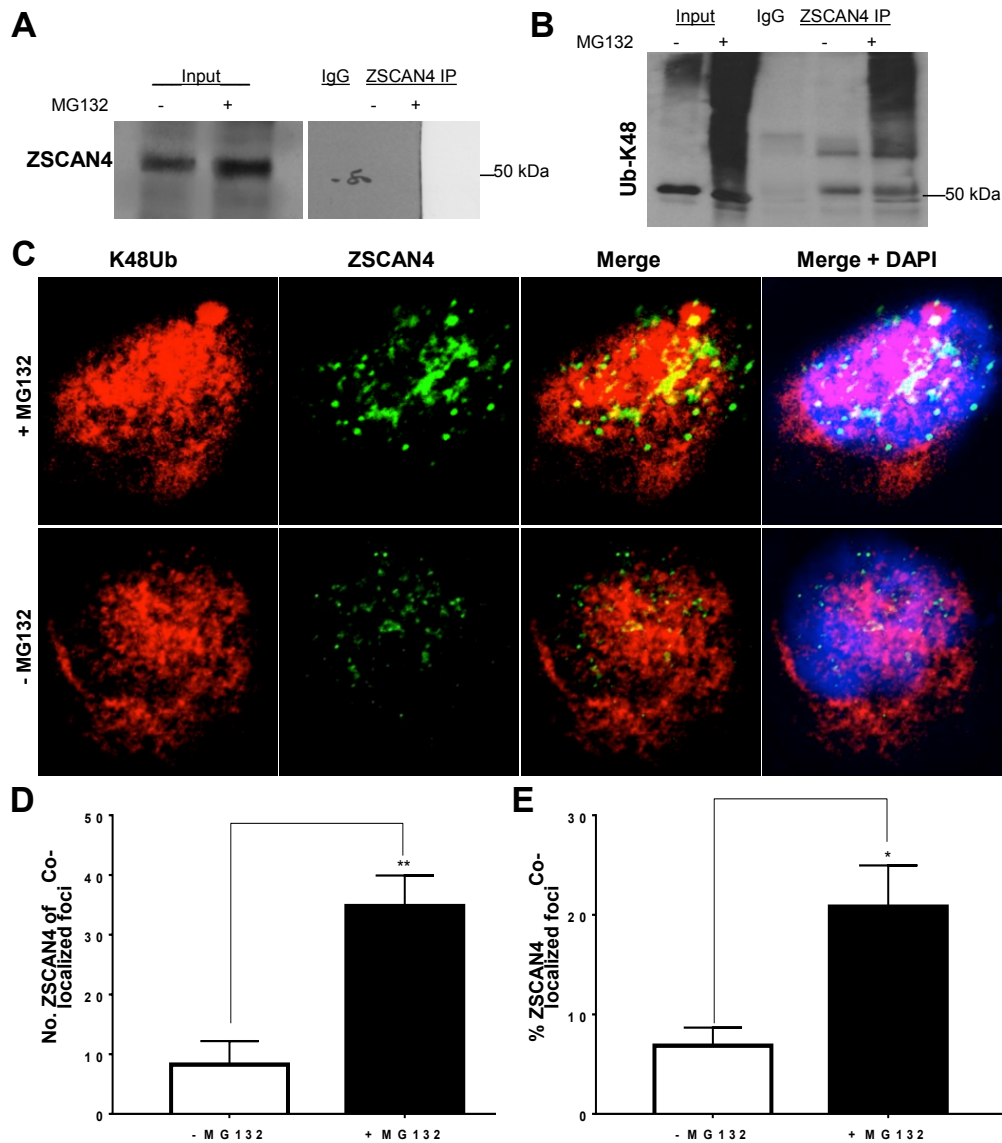


Figure 3.3 ZSCAN4 is ubiquitinated on Lysine 48 (K48Ub) **A.** ZSCAN4 pull down assay by immunoprecipitation (IP) of endogenous ZSCAN4 followed by ZSCAN4 immunoblot. **B.** Denaturing conditions were used to demonstrate covalently bound ubiquitin followed by ZSCAN4-IP and immunoblot with Lysine 48 specific ubiquitin antibody (anti-K48Ub). MG132 treated and cells indicate that ZSCAN4 is polyubiquitinated. Untreated cells were used as controls. **C.** Representative images of confocal microscopy analysis showing co-immunostaining in Tu167 wild type (WT) cells treated with MG132 (+MG132) or untreated (-MG132) controls using anti-ZSCAN4 (green) and anti-K48 ubiquitin (red) indicates the ubiquitinated form of ZSCAN4 co-localizes with K48Ub, suggesting its degradation in proteasomes. **D.** Colocalization analyses with ImageJ show an increase in the number of ZSCAN4 foci colocalized with K48Ub and **E.** the % of ZSCAN4 foci colocalized with K48Ub based on centers of mass-particles coincidence following treatment with MG132 (+MG132) compared to untreated isogenic control cells (Tu167). (n=6 per group and average of >300 foci analyzed per group.) Asterisks indicate * p<0.05, ** p<0.01.

3.3.4 The E3 ubiquitin ligase RNF20 negative regulates ZSCAN4 protein stability

To further characterize the ZSCAN4 ubiquitination mechanism, we performed ZSCAN4 immunoprecipitation (IP) followed by mass spectrometry. Ranking atop the list of interacting proteins, we found the E3 ubiquitin ligase RNF20. Co-IP for ZSCAN4 followed by RNF20 immunoblot validates that ZSCAN4 associates with RNF20 (**Fig 3.4A**). Immunofluorescence staining followed by confocal microscopy confirm the co-localization between ZSCAN4 and RNF20, which also increases after ZSCAN4 induction (**Fig 3.4B**).

RNF20, also known as BRE1, is an E3 ubiquitin ligase that has been implicated in protein degradation [177]. Therefore, we next sought to study the effect of RNF20 depletion on ZSCAN4 protein stability. WT Tu167 cells were transfected with RNF20 RNAi (siRNA) for 48h and compared to isogenic cells transfected with non-targeting control (NTC-siRNA). Interestingly, our immunoblot analyses reveal that depletion of RNF20 by SMARTpool siRNA, or independently by two different RNF20 siRNA sequences, results in an increase in ZSCAN4 protein when compared to NTC-siRNA (**Fig 3.4C**). Conversely, our quantitative reverse transcription PCR (qRT-PCR) analysis in the RNF20 knockdown cells excludes transcriptional regulation of ZSCAN4 by RNF20 (**Fig 3.4D**). These results were validated in multiple independent experiments in triplicates and suggest that RNF20 regulates ZSCAN4 levels in a post-translational manner.

To determine the effect of RNF20 depletion on ZSCAN4 half-life, we performed protein half-life analysis by CHX following RNF20 knockdown (pool siRNA) in WT Tu167 cells. As expected, the half-life of ZSCAN4 remains at 8.1h in NTC-siRNA

transfected cells (**Fig 3.4E, F**). However, our data indicate that RNF20 knockdown stabilizes ZSCAN4, as protein levels remained stable for the entire duration of the assay (10h) (**Fig 3.4G, H**). Data was reproduced in three independent experiments (n=3; $p<0.001$). These results suggest that RNF20 depletion leads to accumulation of ZSCAN4 protein and indicate that RNF20 negatively regulates ZSCAN4 protein stability.

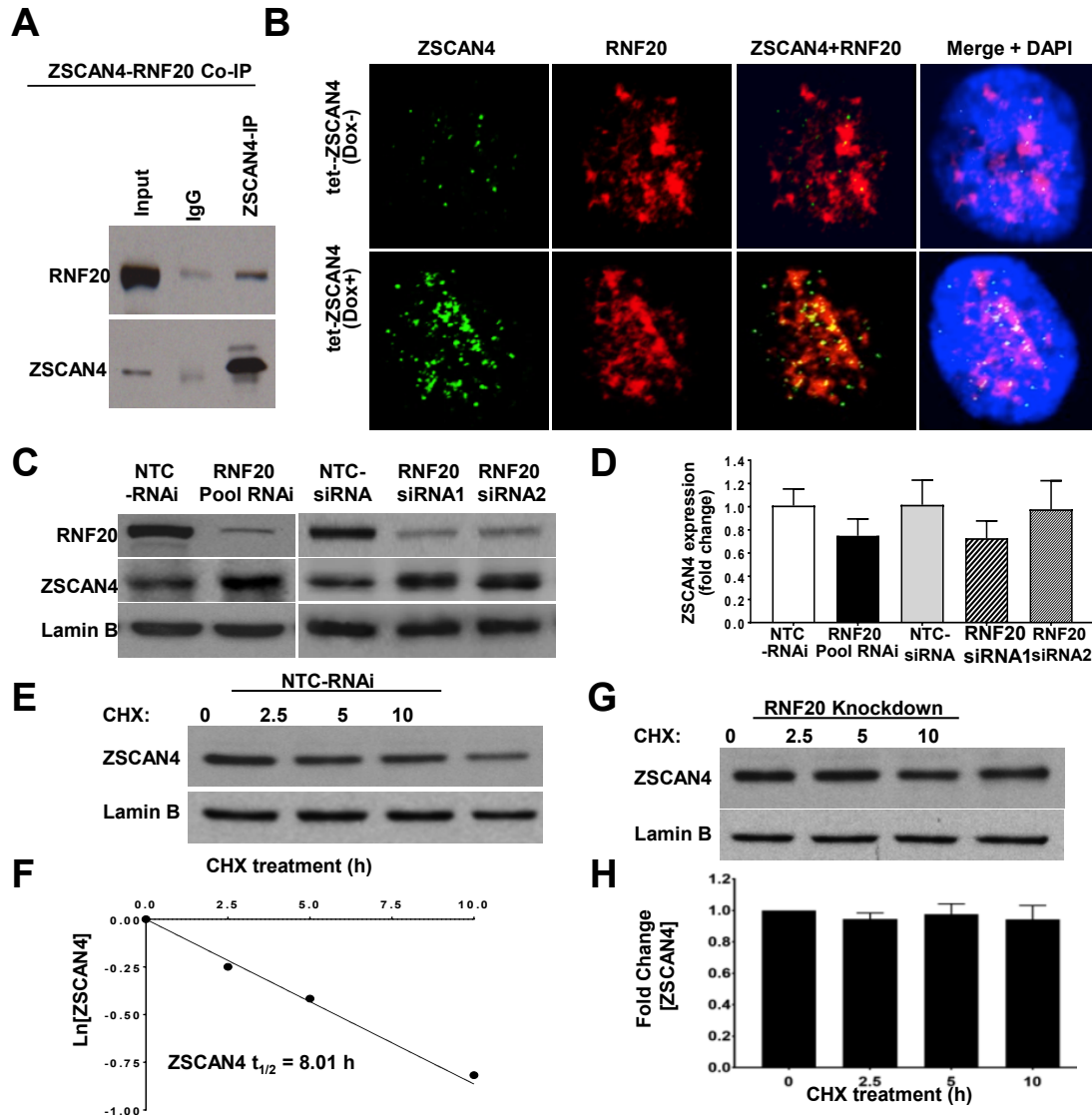


Figure 3.4 The E3 ubiquitin ligase RNF20 negatively regulates and interacts with ZSCAN4 **A.** Co-IP of ZSCAN4 and immunoblot with anti-RNF20 displays interaction. **B.** Confocal microscope images in untreated tet-ZSCAN4 cells (Dox-) show co-localization of RNF20 (red) and ZSCAN4 (green). DNA is stained with DAPI (blue). Furthermore, co-localization increases following ZSCAN4 induction (Dox+). **C.** Immunoblot analyses show successful RNF20 knockdown by SMARTpool siRNA and two different siRNA (RNAi 1 and RNAi 2) compared to non-template controls (NTC). Conversely, RNF20 depletion results in a significant increase in ZSCAN4. **D.** qRT-PCR analysis in RNF20 depleted by the indicated siRNAs show no significant change in ZSCAN4 expression compared to NTC-siRNA controls. **E-F.** Protein half-life analyses after treatment with CHX and immunoblot with corresponding antibodies indicate that NTC-siRNA do not alter the ZSCAN4 protein half-life which remains about 8 h, yet, as shown in **G-H.** Knockdown of RNF20 (pool siRNA) leads to stabilization of ZSCAN4 protein. All data shown represent three independent experiments.

3.4 Discussion

ZSCAN4 plays a critical role in ES telomere regulation and genomic stability. ZSCAN4 has been indicated as a nuclear reprogramming factor [9], and only a short induction improves the developmental potency of ES cells. Previous reports have suggested that the human ZSCAN4 is aberrantly activated in cancer [200], and interacts with the shelterin components important for telomere stability [16, 217]. However, to date, little is known about ZSCAN4 protein turnover or regulation.

Previous studies have shown that transient ZSCAN4 expression must be tightly controlled in order to exert its important role in preservation of stem cell lifespan. This suggests the importance of regulating ZSCAN4 not just transcriptionally, but more importantly at the protein level. Here we show for the first time, the specific regulation of ZSCAN4 protein turnover and the pathway through which this is achieved. Our ZSCAN4 degradation assay demonstrated that the half-life of ZSCAN4 is 8h. We show that ZSCAN4 is not degraded by autophagy, but instead is regulated by a proteasome dependent pathway. Our data reveal that inhibition of the proteasome results in accumulation of ZSCAN4 in a time and dose dependent manner. Proteins are targeted to the proteasome for degradation by ligation of ubiquitin side chains [154, 219]. Specifically, chains linked through lysine 48 ubiquitination serve as the signal for proteasomal degradation. Our Co-IP assays confirm that ZSCAN4 is lysine 48 polyubiquitinated. These data are further validated by co-localization studies between ZSCAN4 and lysine 48 specific poly-ubiquitin. Thus, we infer that the UPS plays a critical role in modulating ZSCAN4 levels and activity in the cell.

The enzymes responsible for specific ubiquitination of proteins are termed E3 ubiquitin ligases. E3 ubiquitin ligases facilitate the transfer of ubiquitin moieties by bringing E2 ubiquitin conjugating enzymes and substrate into close contact [154]. Our ZSCAN4 pull down assay followed by mass spectrometry identifies RNF20 as an interacting E3 ubiquitin ligase. RNF20, also known as BRE1, has been implicated in epigenetic regulation [172, 220] and as a putative tumor suppressor in cancer [181]. RNF20 was also shown to promote the polyubiquitination and proteasomal degradation of proteins [177]. Our data confirm the interaction between ZSCAN4 and RNF20 through co-immunostaining and co-IP. Importantly, our results show that depletion of RNF20 does not affect ZSCAN4 RNA transcription, yet it leads to the accumulation and stabilization of ZSCAN4 protein, suggesting it as a novel negative regulator of ZSCAN4 protein stability. Due to the important role of ZSCAN4 in the generation of iPS cells, our results have important implications in telomere and genomic stability regulation, stem cell biology, and cancer.

Chapter 4: Conclusions, Perspectives, and Future Directions

4.1 Conclusions

Our results provide important insight into a new mechanism by which CSCs maintain their capacity to self-renew and differentiate into a heterogeneous tumor. This is the first study to report the role of ZSCAN4 in CSCs and our data suggests that ZSCAN4 is a novel regulator of the CSC phenotype.

We found that ZSCAN4 was enriched for and mark the HNSCC CSC population. Remarkably, induction of ZSCAN4 increased the frequency of CSCs within HNSCC cell lines. ZSCAN4 showed similar activity to its homolog in mES cells as induction led to a rapid accumulation of open chromatin marks, many of which were localized to the promoter regions of pluripotency transcription factors. Indeed, ZSCAN4 induction led to increased expression of pluripotency factors and CSC stem cell markers. Furthermore, extreme limiting dilution *in vivo* indicated that ZSCAN4 leads to a significant increase in tumor forming frequency. Thus, we conclude that ZSCAN4 promotes the CSC phenotype.

We further provided evidence that ZSCAN4 is essential in maintaining the CSC phenotype. Knockdown of ZSCAN4 resulted in decreased CSC frequency and self-renewal capability. Loss of ZSCAN4 led to decreased expression of CSC markers and pluripotency factors, as well as increased hypersensitivity to genotoxic drugs. Finally, knockdown of ZSCAN4 resulted in decreased tumor formation *in vivo*. Thus, ZSCAN4 appears to maintain the CSC population and be required for tumorigenesis *in vivo*. Due to CSC derived tumor recurrence, new therapies targeting CSC factors are increasingly

entering the clinic. As its knockdown resulted in decreased CSC maintenance and increased sensitivity to conventional cancer drugs, ZSCAN4 is an attractive therapeutic target.

Given the significance of ZSCAN4 as a critical cancer stemness factor, we next chose to analyze ZSCAN4 protein turnover in cancer cells. Prior studies reported that ZSCAN4 transcription is tightly regulated, but did not explore regulation of ZSCAN4 protein. Our results provide insight into the pathway and mediators that regulate ZSCAN4 protein levels in human cancer cells. We determined the half-life of ZSCAN4 protein to be 8.0 hours. Interestingly, we found that ZSCAN4 is not degraded through the autophagic pathway but via the ubiquitin proteasome system. ZSCAN4 is lysine 48 polyubiquitinated, a signal for proteasomal degradation. We provided evidence that ZSCAN4 interacts with the E3 ubiquitin ligase RNF20, a putative tumor suppressor that plays a role in protein degradation and cellular differentiation. Further, we demonstrated that RNF20 negatively regulates ZSCAN4 protein stability, as knockdown stabilizes ZSCAN4 levels. As RNF20 has been reported to mediate cancer suppression, analysis of ZSCAN4 and RNF20 protein levels could be of diagnostic and prognostic value for cancer patients.

4.2 Outstanding Questions and Future Directions

4.2.1 How is ZSCAN4 expression regulated in CSCs?

Our data show that ZSCAN4 protein turnover is controlled through the UPS and regulated by the E3 ubiquitin ligase RNF20 (See Chapter 3). We also demonstrated that ZSCAN4 expression is increased during spheroid formation through use of our reporter construct. While ZSCAN4 expression is well characterized during embryonic

development and in mES cells, there is still little known of the factors that control ZSCAN4 expression in cancer and CSCs [221-223].

ZSCAN4 is expressed during the 2-cell stage in mouse embryogenesis and subsequently quickly shut down, suggesting tight control [2]. In mES cells, ZSCAN4 expression is brief and limited to a small fraction of the cells at a given time. Evidence suggests that DNA damaging agents and the PI3-Kinase pathway regulate ZSCAN4 expression in mES cells [12]. Additionally, telomere shortening could activate ZSCAN4 expression through the telomere positioning effect. Due to its localization at the distal end of the q-arm of chromosome 19, telomere shortening could de-compact sub-telomeric chromatin, making the ZSCAN4 promoter more accessible to the transcriptional machinery [224]. While ZSCAN4 expression in adult tissue is low, recent reports suggest that ZSCAN4 is activated in the presence of inflammation. DNA damage, the PI3-Kinase pathway, and inflammation could play a role in ZSCAN4 expression in cancer as they have all been implicated in cancer and cancer stem cells [27].

Data in our cancer cell lines with the ZSCAN4 reporter indicate that ZSCAN4 expression is indeed transient, as 100% positive mCherry/ZSCAN4 cells lose ZSCAN4 expression after 14 days. Further studies into mechanisms regulating the ZSCAN4 promoter in CSCs may elucidate the signaling mechanisms that govern ZSCAN4 transcription.

4.2.2 How does ZSCAN4 facilitate an open chromatin state?

In mES cells, ZSCAN4 expression correlates with a rapid opening and reset of the chromatin state, as demonstrated by an increase of open chromatin marks [9]. Our data in HNSCC shows that induction of ZSCAN4 also results in an increase of open chromatin

marks and correlates with pluripotent expression. However, the mechanism by which ZSCAN4 facilitates these epigenetic changes remains unknown. Through ZSCAN4 pulldown followed by mass spectroscopy, our lab has identified several histone modifying and chromatin remodeling enzymes. Confirmation and functional exploration of these interactions with ZSCAN4 is needed. As ZSCAN4 associated histone acetylation promotes the CSC phenotype, inhibitors of histone acetylating and de-acetylating enzymes currently used in the clinic could potentially destabilize the CSC state [225].

4.2.3 Is ZSCAN4 activity on telomeres mediated through its epigenetic effect on telomeric chromatin?

ZSCAN4 has been predominantly studied in relation to its telomere elongation function [1]. In mES cells, ZSCAN4 localizes to telomeres and promotes their elongation through recombination. ZSCAN4 has been shown to elongate telomeres in induced pluripotent stem cells as well. Interestingly, data from our lab demonstrates that ZSCAN4 promotes telomere elongation in HNSCC [20].

Like any other sequence, telomeric DNA is organized into chromatin, where can fluctuate between an open and closed state [226]. In order for telomere elongation machinery to access the DNA, telomeric chromatin undergoing lengthening typically maintains a more open state. Our data showed that induction of ZSCAN4 promotes a more open chromatin state and some of these open chromatin marks increase at pluripotent gene promoters. However, future work should examine the chromatin dynamics at telomeres after ZSCAN4 induction. Localization of open chromatin marks at telomeres can be assessed by chromatin immunoprecipitation. If increased open marks

localize to telomeres, their necessity in ZSCAN4 mediated telomere elongation can be assessed via inhibition of histone modifying enzymes.

4.2.4 Is ZSCAN4 involved in DNA repair?

A major attribute of CSCs is an increased ability to resist traditional genotoxic therapies. CSCs achieve this through multiple mechanisms, including rapid upregulation of the DNA repair machinery [95]. In mES cells, ZSCAN4 contributes to genome stability and is upregulated in response to DNA damage. Data previously generated by our laboratory demonstrates that ZSCAN4 forms a complex with the DNA double strand break repair enzymes MRE11A and RAD50. These enzymes are involved in two main double strand repair pathways: homologous recombination and non-homologous end joining [227]. Our data in HNSCC demonstrate that ZSCAN4 knockdown cells exhibit hypersensitivity to double strand break inducing chemotherapeutic agents (See Chapter 2). Therefore, ZSCAN4 might play a role in DNA repair. Investigation into ZSCAN4 expression after DNA damage as well as identification of the repair mechanism by which ZSCAN4 functions could potentially provide new avenues of therapeutic intervention in the ZSCAN4 CSC mechanism.

While future efforts will explore the ZSCAN4 mechanism in more depth, the work presented here uncovers a novel role for ZSCAN4 in cancer stemness. With previous work on ZSCAN4 focused in mES cells we have shown that human ZSCAN4 is critical for both the promotion and maintenance of CSCs. We further identified previously undiscovered protein interactions that directly influence ZSCAN4 protein stability and function. Along with limited expression after embryonic development, this

new evidence substantiates pursuing a cancer therapeutic strategy that focuses on targeting the ZSCAN4 pathway.

References

1. Zalzman, M., et al., *Zscan4 regulates telomere elongation and genomic stability in ES cells*. Nature, 2010. **464**(7290): p. 858-63.
2. Falco, G., et al., *Zscan4: a novel gene expressed exclusively in late 2-cell embryos and embryonic stem cells*. Dev Biol, 2007. **307**(2): p. 539-50.
3. Edelstein, L.C. and T. Collins, *The SCAN domain family of zinc finger transcription factors*. Gene, 2005. **359**: p. 1-17.
4. Sander, T.L., et al., *The SCAN domain defines a large family of zinc finger transcription factors*. Gene, 2003. **310**: p. 29-38.
5. Carter, M.G., et al., *An in situ hybridization-based screen for heterogeneously expressed genes in mouse ES cells*. Gene Expr Patterns, 2008. **8**(3): p. 181-98.
6. Rippon, H.J. and A.E. Bishop, *Embryonic stem cells*. Cell Prolif, 2004. **37**(1): p. 23-34.
7. Nakai-Futatsugi, Y. and H. Niwa, *Zscan4 Is Activated after Telomere Shortening in Mouse Embryonic Stem Cells*. Stem Cell Reports, 2016. **6**(4): p. 483-495.
8. Meshorer, E. and T. Misteli, *Chromatin in pluripotent embryonic stem cells and differentiation*. Nat Rev Mol Cell Biol, 2006. **7**(7): p. 540-6.
9. Akiyama, T., et al., *Transient bursts of Zscan4 expression are accompanied by the rapid derepression of heterochromatin in mouse embryonic stem cells*. DNA Res, 2015.
10. Amano, T., et al., *Zscan4 restores the developmental potency of embryonic stem cells*. Nat Commun, 2013. **4**: p. 1966.
11. Dan, J., et al., *Zscan4 Inhibits Maintenance DNA Methylation to Facilitate Telomere Elongation in Mouse Embryonic Stem Cells*. Cell Rep, 2017. **20**(8): p. 1936-1949.
12. Storm, M.P., et al., *Zscan4 is regulated by PI3-kinase and DNA-damaging agents and directly interacts with the transcriptional repressors LSD1 and CtBP2 in mouse embryonic stem cells*. PLoS One, 2014. **9**(3): p. e89821.
13. Takahashi, K. and S. Yamanaka, *Induction of pluripotent stem cells from mouse embryonic and adult fibroblast cultures by defined factors*. Cell, 2006. **126**(4): p. 663-76.
14. Jiang, J., et al., *Zscan4 promotes genomic stability during reprogramming and dramatically improves the quality of iPS cells as demonstrated by tetraploid complementation*. Cell Res, 2013. **23**(1): p. 92-106.
15. Hirata, T., et al., *Zscan4 transiently reactivates early embryonic genes during the generation of induced pluripotent stem cells*. Sci Rep, 2012. **2**: p. 208.
16. Lee, K. and L.S. Gollahon, *Zscan4 interacts directly with human Rap1 in cancer cells regardless of telomerase status*. Cancer Biol Ther, 2014. **15**(8): p. 1094-105.
17. Kunicka, Z., I. Mucha, and J. Fajkus, *Telomerase activity in head and neck cancer*. Anticancer Res, 2008. **28**(5B): p. 3125-9.
18. Bryan, T.M., et al., *Evidence for an alternative mechanism for maintaining telomere length in human tumors and tumor-derived cell lines*. Nat Med, 1997. **3**(11): p. 1271-4.
19. Liu, A., X. Yu, and S. Liu, *Pluripotency transcription factors and cancer stem cells: small genes make a big difference*. Chin J Cancer, 2013. **32**(9): p. 483-7.

20. Meltzer, W.A., *A Novel Regulator of Telomere Length in Cancer*, in *Biochemistry and Molecular Biology* 2017, University of Maryland, Baltimore: Baltimore, MD.
21. Vermeulen, L., et al., *The developing cancer stem-cell model: clinical challenges and opportunities*. *Lancet Oncol*, 2012. **13**(2): p. e83-9.
22. Fulawka, L., P. Donizy, and A. Halon, *Cancer stem cells--the current status of an old concept: literature review and clinical approaches*. *Biol Res*, 2014. **47**: p. 66.
23. Rich, J.N., *Cancer stem cells: understanding tumor hierarchy and heterogeneity*. *Medicine (Baltimore)*, 2016. **95**(1 Suppl 1): p. S2-7.
24. Gerlinger, M., et al., *Intratour heterogeneity in urologic cancers: from molecular evidence to clinical implications*. *Eur Urol*, 2015. **67**(4): p. 729-37.
25. Marusyk, A. and K. Polyak, *Tumor heterogeneity: causes and consequences*. *Biochim Biophys Acta*, 2010. **1805**(1): p. 105-17.
26. Reya, T., et al., *Stem cells, cancer, and cancer stem cells*. *Nature*, 2001. **414**(6859): p. 105-11.
27. Lobo, N.A., et al., *The biology of cancer stem cells*. *Annu Rev Cell Dev Biol*, 2007. **23**: p. 675-99.
28. Wang, W., et al., *Dynamics between cancer cell subpopulations reveals a model coordinating with both hierarchical and stochastic concepts*. *PLoS One*, 2014. **9**(1): p. e84654.
29. Clevers, H., *The cancer stem cell: premises, promises and challenges*. *Nat Med*, 2011. **17**(3): p. 313-9.
30. Nowell, P.C., *The clonal evolution of tumor cell populations*. *Science*, 1976. **194**(4260): p. 23-8.
31. Uckun, F.M., et al., *Leukemic cell growth in SCID mice as a predictor of relapse in high-risk B-lineage acute lymphoblastic leukemia*. *Blood*, 1995. **85**(4): p. 873-8.
32. Al-Hajj, M., et al., *Prospective identification of tumorigenic breast cancer cells*. *Proc Natl Acad Sci U S A*, 2003. **100**(7): p. 3983-8.
33. Singh, S.K., et al., *Identification of human brain tumour initiating cells*. *Nature*, 2004. **432**(7015): p. 396-401.
34. Dalerba, P., et al., *Phenotypic characterization of human colorectal cancer stem cells*. *Proc Natl Acad Sci U S A*, 2007. **104**(24): p. 10158-63.
35. Alamgeer, M., et al., *Cancer stem cells in lung cancer: Evidence and controversies*. *Respirology*, 2013. **18**(5): p. 757-64.
36. Maitland, N.J. and A.T. Collins, *Prostate cancer stem cells: a new target for therapy*. *J Clin Oncol*, 2008. **26**(17): p. 2862-70.
37. Prince, M.E., et al., *Identification of a subpopulation of cells with cancer stem cell properties in head and neck squamous cell carcinoma*. *Proc Natl Acad Sci U S A*, 2007. **104**(3): p. 973-8.
38. Schatton, T., et al., *Identification of cells initiating human melanomas*. *Nature*, 2008. **451**(7176): p. 345-9.
39. Zhang, S., et al., *Identification and characterization of ovarian cancer-initiating cells from primary human tumors*. *Cancer Res*, 2008. **68**(11): p. 4311-20.
40. Wicha, M.S., S. Liu, and G. Dontu, *Cancer stem cells: an old idea--a paradigm shift*. *Cancer Res*, 2006. **66**(4): p. 1883-90; discussion 1895-6.
41. Lapidot, T., et al., *A cell initiating human acute myeloid leukaemia after transplantation into SCID mice*. *Nature*, 1994. **367**(6464): p. 645-8.
42. Takaishi, S., et al., *Identification of gastric cancer stem cells using the cell surface marker CD44*. *Stem Cells*, 2009. **27**(5): p. 1006-20.

43. Yang, Z.F., et al., *Significance of CD90+ cancer stem cells in human liver cancer*. *Cancer Cell*, 2008. **13**(2): p. 153-66.
44. Li, C., et al., *Identification of pancreatic cancer stem cells*. *Cancer Res*, 2007. **67**(3): p. 1030-7.
45. Ricci-Vitiani, L., et al., *Identification and expansion of human colon-cancer-initiating cells*. *Nature*, 2007. **445**(7123): p. 111-5.
46. Collins, A.T., et al., *Prospective identification of tumorigenic prostate cancer stem cells*. *Cancer Res*, 2005. **65**(23): p. 10946-51.
47. Bertolini, G., et al., *Highly tumorigenic lung cancer CD133+ cells display stem-like features and are spared by cisplatin treatment*. *Proc Natl Acad Sci U S A*, 2009. **106**(38): p. 16281-6.
48. Zhang, C., et al., *Identification of CD44+CD24+ gastric cancer stem cells*. *J Cancer Res Clin Oncol*, 2011. **137**(11): p. 1679-86.
49. He, J., et al., *CD90 is identified as a candidate marker for cancer stem cells in primary high-grade gliomas using tissue microarrays*. *Mol Cell Proteomics*, 2012. **11**(6): p. M111010744.
50. Ginestier, C., et al., *ALDH1 is a marker of normal and malignant human mammary stem cells and a predictor of poor clinical outcome*. *Cell Stem Cell*, 2007. **1**(5): p. 555-67.
51. Golebiewska, A., et al., *Critical appraisal of the side population assay in stem cell and cancer stem cell research*. *Cell Stem Cell*, 2011. **8**(2): p. 136-47.
52. Shaheen, S., et al., *Spheroid-Formation (Colonosphere) Assay for in Vitro Assessment and Expansion of Stem Cells in Colon Cancer*. *Stem Cell Rev*, 2016. **12**(4): p. 492-9.
53. Matsui, W.H., *Cancer stem cell signaling pathways*. *Medicine (Baltimore)*, 2016. **95**(1 Suppl 1): p. S8-S19.
54. Stine, R.R. and E.L. Matunis, *JAK-STAT signaling in stem cells*. *Adv Exp Med Biol*, 2013. **786**: p. 247-67.
55. Birnie, R., et al., *Gene expression profiling of human prostate cancer stem cells reveals a pro-inflammatory phenotype and the importance of extracellular matrix interactions*. *Genome Biol*, 2008. **9**(5): p. R83.
56. Zhou, J., et al., *Activation of the PTEN/mTOR/STAT3 pathway in breast cancer stem-like cells is required for viability and maintenance*. *Proc Natl Acad Sci U S A*, 2007. **104**(41): p. 16158-63.
57. Abel, E.V., et al., *The Notch pathway is important in maintaining the cancer stem cell population in pancreatic cancer*. *PLoS One*, 2014. **9**(3): p. e91983.
58. Holland, J.D., et al., *Wnt signaling in stem and cancer stem cells*. *Curr Opin Cell Biol*, 2013. **25**(2): p. 254-64.
59. Polakis, P., *Wnt signaling in cancer*. *Cold Spring Harb Perspect Biol*, 2012. **4**(5).
60. Merchant, A.A. and W. Matsui, *Targeting Hedgehog--a cancer stem cell pathway*. *Clin Cancer Res*, 2010. **16**(12): p. 3130-40.
61. Bahena-Ocampo, I., et al., *miR-10b expression in breast cancer stem cells supports self-renewal through negative PTEN regulation and sustained AKT activation*. *EMBO Rep*, 2016. **17**(7): p. 1081.
62. Liu, M., et al., *The canonical NF-kappaB pathway governs mammary tumorigenesis in transgenic mice and tumor stem cell expansion*. *Cancer Res*, 2010. **70**(24): p. 10464-73.
63. Lathia, J.D., et al., *Deadly teamwork: neural cancer stem cells and the tumor microenvironment*. *Cell Stem Cell*, 2011. **8**(5): p. 482-5.
64. Solter, D., *From teratocarcinomas to embryonic stem cells and beyond: a history of embryonic stem cell research*. *Nat Rev Genet*, 2006. **7**(4): p. 319-27.

65. Loh, Y.H., et al., *The Oct4 and Nanog transcription network regulates pluripotency in mouse embryonic stem cells*. Nat Genet, 2006. **38**(4): p. 431-40.
66. Chiou, S.H., et al., *Positive correlations of Oct-4 and Nanog in oral cancer stem-like cells and high-grade oral squamous cell carcinoma*. Clin Cancer Res, 2008. **14**(13): p. 4085-95.
67. Santini, R., et al., *SOX2 regulates self-renewal and tumorigenicity of human melanoma-initiating cells*. Oncogene, 2014. **33**(38): p. 4697-708.
68. Jeter, C.R., et al., *NANOG promotes cancer stem cell characteristics and prostate cancer resistance to androgen deprivation*. Oncogene, 2011. **30**(36): p. 3833-45.
69. Zbinden, M., et al., *NANOG regulates glioma stem cells and is essential in vivo acting in a cross-functional network with GLI1 and p53*. EMBO J, 2010. **29**(15): p. 2659-74.
70. Zhou, X., et al., *Expression of the stem cell marker, Nanog, in human endometrial adenocarcinoma*. Int J Gynecol Pathol, 2011. **30**(3): p. 262-70.
71. Yu, F., et al., *Kruppel-like factor 4 (KLF4) is required for maintenance of breast cancer stem cells and for cell migration and invasion*. Oncogene, 2011. **30**(18): p. 2161-72.
72. Hadjimichael, C., et al., *Common stemness regulators of embryonic and cancer stem cells*. World J Stem Cells, 2015. **7**(9): p. 1150-84.
73. Azuara, V., et al., *Chromatin signatures of pluripotent cell lines*. Nat Cell Biol, 2006. **8**(5): p. 532-8.
74. Giudice, F.S., et al., *Inhibition of histone deacetylase impacts cancer stem cells and induces epithelial-mesenchyme transition of head and neck cancer*. PLoS One, 2013. **8**(3): p. e58672.
75. Allegra, E., et al., *The role of BMI1 as a biomarker of cancer stem cells in head and neck cancer: a review*. Oncology, 2014. **86**(4): p. 199-205.
76. Adhikary, G., et al., *Survival of skin cancer stem cells requires the Ezh2 polycomb group protein*. Carcinogenesis, 2015. **36**(7): p. 800-10.
77. Morita, R., et al., *DNA methyltransferase 1 is essential for initiation of the colon cancers*. Exp Mol Pathol, 2013. **94**(2): p. 322-9.
78. Yu, F., et al., *Mir-30 reduction maintains self-renewal and inhibits apoptosis in breast tumor-initiating cells*. Oncogene, 2010. **29**(29): p. 4194-204.
79. Gutschner, T., et al., *The noncoding RNA MALAT1 is a critical regulator of the metastasis phenotype of lung cancer cells*. Cancer Res, 2013. **73**(3): p. 1180-9.
80. Carew, J.S., F.J. Giles, and S.T. Nawrocki, *Histone deacetylase inhibitors: mechanisms of cell death and promise in combination cancer therapy*. Cancer Lett, 2008. **269**(1): p. 7-17.
81. Plimack, E.R., D.J. Stewart, and J.P. Issa, *Combining epigenetic and cytotoxic therapy in the treatment of solid tumors*. J Clin Oncol, 2007. **25**(29): p. 4519-21.
82. Mani, S.A., et al., *The epithelial-mesenchymal transition generates cells with properties of stem cells*. Cell, 2008. **133**(4): p. 704-15.
83. Thiery, J.P., et al., *Epithelial-mesenchymal transitions in development and disease*. Cell, 2009. **139**(5): p. 871-90.
84. Chiou, S.H., et al., *Coexpression of Oct4 and Nanog enhances malignancy in lung adenocarcinoma by inducing cancer stem cell-like properties and epithelial-mesenchymal transdifferentiation*. Cancer Res, 2010. **70**(24): p. 10433-44.
85. Kramer, N., et al., *In vitro cell migration and invasion assays*. Mutat Res, 2013. **752**(1): p. 10-24.
86. Ota, I., et al., *Induction of a MT1-MMP and MT2-MMP-dependent basement membrane transmigration program in cancer cells by Snail1*. Proc Natl Acad Sci U S A, 2009. **106**(48): p. 20318-23.

87. Miles, F.L., et al., *Stepping out of the flow: capillary extravasation in cancer metastasis*. Clin Exp Metastasis, 2008. **25**(4): p. 305-24.
88. Stoletov, K., et al., *Visualizing extravasation dynamics of metastatic tumor cells*. J Cell Sci, 2010. **123**(Pt 13): p. 2332-41.
89. Pattabiraman, D.R. and R.A. Weinberg, *Tackling the cancer stem cells - what challenges do they pose?* Nat Rev Drug Discov, 2014. **13**(7): p. 497-512.
90. Cojoc, M., et al., *A role for cancer stem cells in therapy resistance: cellular and molecular mechanisms*. Semin Cancer Biol, 2015. **31**: p. 16-27.
91. Essers, M.A. and A. Trumpp, *Targeting leukemic stem cells by breaking their dormancy*. Mol Oncol, 2010. **4**(5): p. 443-50.
92. Chow, E.K., et al., *Oncogene-specific formation of chemoresistant murine hepatic cancer stem cells*. Hepatology, 2012. **56**(4): p. 1331-41.
93. Duong, H.Q., et al., *Aldehyde dehydrogenase 1A1 confers intrinsic and acquired resistance to gemcitabine in human pancreatic adenocarcinoma MIA PaCa-2 cells*. Int J Oncol, 2012. **41**(3): p. 855-61.
94. Konopleva, M., et al., *The anti-apoptotic genes Bcl-X(L) and Bcl-2 are over-expressed and contribute to chemoresistance of non-proliferating leukaemic CD34+ cells*. Br J Haematol, 2002. **118**(2): p. 521-34.
95. Bao, S., et al., *Glioma stem cells promote radioresistance by preferential activation of the DNA damage response*. Nature, 2006. **444**(7120): p. 756-60.
96. Wilson, B.J., et al., *ABCB5 identifies a therapy-refractory tumor cell population in colorectal cancer patients*. Cancer Res, 2011. **71**(15): p. 5307-16.
97. Vinogradov, S. and X. Wei, *Cancer stem cells and drug resistance: the potential of nanomedicine*. Nanomedicine (Lond), 2012. **7**(4): p. 597-615.
98. Takebe, N., et al., *Targeting cancer stem cells by inhibiting Wnt, Notch, and Hedgehog pathways*. Nat Rev Clin Oncol, 2011. **8**(2): p. 97-106.
99. Abubaker, K., et al., *Inhibition of the JAK2/STAT3 pathway in ovarian cancer results in the loss of cancer stem cell-like characteristics and a reduced tumor burden*. BMC Cancer, 2014. **14**: p. 317.
100. Chen, B., et al., *Small molecule-mediated disruption of Wnt-dependent signaling in tissue regeneration and cancer*. Nature Chemical Biology, 2009. **5**(2): p. 100-7.
101. Olson, R.E. and C.F. Albright, *Recent progress in the medicinal chemistry of gamma-secretase inhibitors*. Curr Top Med Chem, 2008. **8**(1): p. 17-33.
102. Karthikeyan, S. and S.L. Hoti, *Development of Fourth Generation ABC Inhibitors from Natural Products: A Novel Approach to Overcome Cancer Multidrug Resistance*. Anticancer Agents Med Chem, 2015. **15**(5): p. 605-15.
103. Fukumoto, Y., *Radiosensitization of cancer stem cells in glioblastoma by the simultaneous inhibition of parallel DNA damage response pathways*. Ann Transl Med, 2017. **5**(Suppl 1): p. S2.
104. Nervi, B., et al., *Chemosensitization of acute myeloid leukemia (AML) following mobilization by the CXCR4 antagonist AMD3100*. Blood, 2009. **113**(24): p. 6206-14.
105. Prager, G.W., et al., *Angiogenesis in cancer: Anti-VEGF escape mechanisms*. Transl Lung Cancer Res, 2012. **1**(1): p. 14-25.
106. Munster, P.N., et al., *The histone deacetylase inhibitor suberoylanilide hydroxamic acid induces differentiation of human breast cancer cells*. Cancer Res, 2001. **61**(23): p. 8492-7.
107. Pardoll, D.M., *The blockade of immune checkpoints in cancer immunotherapy*. Nat Rev Cancer, 2012. **12**(4): p. 252-64.

108. Dragu, D.L., et al., *Therapies targeting cancer stem cells: Current trends and future challenges*. World J Stem Cells, 2015. **7**(9): p. 1185-201.
109. Chang, J.C., *Cancer stem cells: Role in tumor growth, recurrence, metastasis, and treatment resistance*. Medicine (Baltimore), 2016. **95**(1 Suppl 1): p. S20-5.
110. Marur, S. and A.A. Forastiere, *Head and Neck Squamous Cell Carcinoma: Update on Epidemiology, Diagnosis, and Treatment*. Mayo Clin Proc, 2016. **91**(3): p. 386-96.
111. Joshi, P., et al., *Head and neck cancers in developing countries*. Rambam Maimonides Med J, 2014. **5**(2): p. e0009.
112. Rothenberg, S.M. and L.W. Ellisen, *The molecular pathogenesis of head and neck squamous cell carcinoma*. J Clin Invest, 2012. **122**(6): p. 1951-7.
113. Ram, H., et al., *Oral cancer: risk factors and molecular pathogenesis*. J Maxillofac Oral Surg, 2011. **10**(2): p. 132-7.
114. Park, B.J., S.I. Chiosea, and J.R. Grandis, *Molecular changes in the multistage pathogenesis of head and neck cancer*. Cancer Biomark, 2010. **9**(1-6): p. 325-39.
115. Klein, J.D. and J.R. Grandis, *The molecular pathogenesis of head and neck cancer*. Cancer Biol Ther, 2010. **9**(1): p. 1-7.
116. American Cancer Society. *Oral Cavity and Oropharyngeal Cancer Stages*. 2017; Available from: <https://www.cancer.org/cancer/oral-cavity-and-oropharyngeal-cancer/detection-diagnosis-staging/staging.html>.
117. Leemans, C.R., B.J. Braakhuis, and R.H. Brakenhoff, *The molecular biology of head and neck cancer*. Nat Rev Cancer, 2011. **11**(1): p. 9-22.
118. Reyes-Gibby, C.C., et al., *Survival patterns in squamous cell carcinoma of the head and neck: pain as an independent prognostic factor for survival*. J Pain, 2014. **15**(10): p. 1015-22.
119. Forastiere, A., et al., *Head and neck cancer*. N Engl J Med, 2001. **345**(26): p. 1890-900.
120. Seiwert, T.Y. and E.E. Cohen, *State-of-the-art management of locally advanced head and neck cancer*. Br J Cancer, 2005. **92**(8): p. 1341-8.
121. Sacco, A.G. and E.E. Cohen, *Current Treatment Options for Recurrent or Metastatic Head and Neck Squamous Cell Carcinoma*. J Clin Oncol, 2015. **33**(29): p. 3305-13.
122. Oliveira, L.R., et al., *CD44+/CD133+ immunophenotype and matrix metalloproteinase-9: Influence on prognosis in early-stage oral squamous cell carcinoma*. Head Neck, 2014. **36**(12): p. 1718-26.
123. Fukusumi, T., et al., *CD10 as a novel marker of therapeutic resistance and cancer stem cells in head and neck squamous cell carcinoma*. Br J Cancer, 2014. **111**(3): p. 506-14.
124. Chen, Y.C., et al., *Aldehyde dehydrogenase 1 is a putative marker for cancer stem cells in head and neck squamous cancer*. Biochem Biophys Res Commun, 2009. **385**(3): p. 307-13.
125. Zhang, P., et al., *Side population in oral squamous cell carcinoma possesses tumor stem cell phenotypes*. Cancer Lett, 2009. **277**(2): p. 227-34.
126. Nor, C., et al., *Cisplatin induces Bmi-1 and enhances the stem cell fraction in head and neck cancer*. Neoplasia, 2014. **16**(2): p. 137-46.
127. Tsai, L.L., et al., *Markedly increased Oct4 and Nanog expression correlates with cisplatin resistance in oral squamous cell carcinoma*. J Oral Pathol Med, 2011. **40**(8): p. 621-8.
128. Dalley, A.J., et al., *Organotypic culture of normal, dysplastic and squamous cell carcinoma-derived oral cell lines reveals loss of spatial regulation of CD44 and p75 NTR in malignancy*. J Oral Pathol Med, 2013. **42**(1): p. 37-46.
129. Chen, C., et al., *Evidence for epithelial-mesenchymal transition in cancer stem cells of head and neck squamous cell carcinoma*. PLoS One, 2011. **6**(1): p. e16466.

130. Baillie, R., et al., *Cancer stem cells in moderately differentiated oral tongue squamous cell carcinoma*. J Clin Pathol, 2016. **69**(8): p. 742-4.
131. Pozzi, V., et al., *Identification and characterization of cancer stem cells from head and neck squamous cell carcinoma cell lines*. Cell Physiol Biochem, 2015. **36**(2): p. 784-98.
132. Lee, H.J., et al., *Positive expression of NANOG, mutant p53, and CD44 is directly associated with clinicopathological features and poor prognosis of oral squamous cell carcinoma*. BMC Oral Health, 2015. **15**(1): p. 153.
133. Chen, D., et al., *Targeting BMI1(+) Cancer Stem Cells Overcomes Chemoresistance and Inhibits Metastases in Squamous Cell Carcinoma*. Cell Stem Cell, 2017. **20**(5): p. 621-634 e6.
134. Reinstein, E. and A. Ciechanover, *Narrative review: protein degradation and human diseases: the ubiquitin connection*. Ann Intern Med, 2006. **145**(9): p. 676-84.
135. Ciechanover, A., *Proteolysis: from the lysosome to ubiquitin and the proteasome*. Nat Rev Mol Cell Biol, 2005. **6**(1): p. 79-87.
136. Korolchuk, V.I., F.M. Menzies, and D.C. Rubinsztein, *Mechanisms of cross-talk between the ubiquitin-proteasome and autophagy-lysosome systems*. FEBS Lett, 2010. **584**(7): p. 1393-8.
137. Ohsumi, Y., *Protein turnover*. IUBMB Life, 2006. **58**(5-6): p. 363-9.
138. Goldberg, A.L., *Protein degradation and protection against misfolded or damaged proteins*. Nature, 2003. **426**(6968): p. 895-9.
139. Chen, Z.J. and L.J. Sun, *Nonproteolytic functions of ubiquitin in cell signaling*. Mol Cell, 2009. **33**(3): p. 275-86.
140. Ciechanover, A. and P. Brundin, *The ubiquitin proteasome system in neurodegenerative diseases: sometimes the chicken, sometimes the egg*. Neuron, 2003. **40**(2): p. 427-46.
141. Tanaka, K., et al., *Ubiquitin, proteasome and parkin*. Biochim Biophys Acta, 2004. **1695**(1-3): p. 235-47.
142. Matsuura, T., et al., *De novo truncating mutations in E6-AP ubiquitin-protein ligase gene (UBE3A) in Angelman syndrome*. Nat Genet, 1997. **15**(1): p. 74-7.
143. Hansson, J.H., et al., *Hypertension caused by a truncated epithelial sodium channel gamma subunit: genetic heterogeneity of Liddle syndrome*. Nat Genet, 1995. **11**(1): p. 76-82.
144. Ohta, T. and M. Fukuda, *Ubiquitin and breast cancer*. Oncogene, 2004. **23**(11): p. 2079-88.
145. Hinkson, I.V. and J.E. Elias, *The dynamic state of protein turnover: It's about time*. Trends Cell Biol, 2011. **21**(5): p. 293-303.
146. Zhou, P., *Determining protein half-lives*. Methods Mol Biol, 2004. **284**: p. 67-77.
147. Yang, Z. and D.J. Klionsky, *Mammalian autophagy: core molecular machinery and signaling regulation*. Curr Opin Cell Biol, 2010. **22**(2): p. 124-31.
148. Glick, D., S. Barth, and K.F. Macleod, *Autophagy: cellular and molecular mechanisms*. J Pathol, 2010. **221**(1): p. 3-12.
149. Mizushima, N., *Autophagy: process and function*. Genes Dev, 2007. **21**(22): p. 2861-73.
150. Eskelinen, E.L. and P. Saftig, *Autophagy: a lysosomal degradation pathway with a central role in health and disease*. Biochim Biophys Acta, 2009. **1793**(4): p. 664-73.
151. Yu, L., Y. Chen, and S.A. Tooze, *Autophagy pathway: Cellular and molecular mechanisms*. Autophagy, 2017: p. 1-9.
152. Mizushima, N., T. Yoshimori, and B. Levine, *Methods in mammalian autophagy research*. Cell, 2010. **140**(3): p. 313-26.

153. Rusten, T.E. and H. Stenmark, *p62, an autophagy hero or culprit?* Nat Cell Biol, 2010. **12**(3): p. 207-9.
154. Nandi, D., et al., *The ubiquitin-proteasome system.* J Biosci, 2006. **31**(1): p. 137-55.
155. Hershko, A. and A. Ciechanover, *The ubiquitin system.* Annu Rev Biochem, 1998. **67**: p. 425-79.
156. Huang, Q. and M.E. Figueiredo-Pereira, *Ubiquitin/proteasome pathway impairment in neurodegeneration: therapeutic implications.* Apoptosis, 2010. **15**(11): p. 1292-311.
157. Al-Hakim, A., et al., *The ubiquitous role of ubiquitin in the DNA damage response.* DNA Repair (Amst), 2010. **9**(12): p. 1229-40.
158. Bedford, L., et al., *Assembly, structure, and function of the 26S proteasome.* Trends Cell Biol, 2010. **20**(7): p. 391-401.
159. Voges, D., P. Zwickl, and W. Baumeister, *The 26S proteasome: a molecular machine designed for controlled proteolysis.* Annu Rev Biochem, 1999. **68**: p. 1015-68.
160. Livneh, I., et al., *The life cycle of the 26S proteasome: from birth, through regulation and function, and onto its death.* Cell Res, 2016. **26**(8): p. 869-85.
161. Smalle, J. and R.D. Vierstra, *The ubiquitin 26S proteasome proteolytic pathway.* Annu Rev Plant Biol, 2004. **55**: p. 555-90.
162. Dahlmann, B., *Role of proteasomes in disease.* BMC Biochem, 2007. **8 Suppl 1**: p. S3.
163. Bedford, L., et al., *Ubiquitin-like protein conjugation and the ubiquitin-proteasome system as drug targets.* Nat Rev Drug Discov, 2011. **10**(1): p. 29-46.
164. Pickart, C.M. and M.J. Eddins, *Ubiquitin: structures, functions, mechanisms.* Biochim Biophys Acta, 2004. **1695**(1-3): p. 55-72.
165. Swatek, K.N. and D. Komander, *Ubiquitin modifications.* Cell Res, 2016. **26**(4): p. 399-422.
166. Ye, Y. and M. Rape, *Building ubiquitin chains: E2 enzymes at work.* Nat Rev Mol Cell Biol, 2009. **10**(11): p. 755-64.
167. Callis, J., *The ubiquitination machinery of the ubiquitin system.* Arabidopsis Book, 2014. **12**: p. e0174.
168. Ardley, H.C. and P.A. Robinson, *E3 ubiquitin ligases.* Essays Biochem, 2005. **41**: p. 15-30.
169. Buetow, L. and D.T. Huang, *Structural insights into the catalysis and regulation of E3 ubiquitin ligases.* Nat Rev Mol Cell Biol, 2016. **17**(10): p. 626-42.
170. Morreale, F.E. and H. Walden, *Types of Ubiquitin Ligases.* Cell, 2016. **165**(1): p. 248-248 e1.
171. Ozkan, E., H. Yu, and J. Deisenhofer, *Mechanistic insight into the allosteric activation of a ubiquitin-conjugating enzyme by RING-type ubiquitin ligases.* Proc Natl Acad Sci U S A, 2005. **102**(52): p. 18890-5.
172. Pavri, R., et al., *Histone H2B monoubiquitination functions cooperatively with FACT to regulate elongation by RNA polymerase II.* Cell, 2006. **125**(4): p. 703-17.
173. Moyal, L., et al., *Requirement of ATM-dependent monoubiquitylation of histone H2B for timely repair of DNA double-strand breaks.* Mol Cell, 2011. **41**(5): p. 529-42.
174. Nakamura, K., et al., *Regulation of homologous recombination by RNF20-dependent H2B ubiquitination.* Mol Cell, 2011. **41**(5): p. 515-28.
175. Pirngruber, J., et al., *CDK9 directs H2B monoubiquitination and controls replication-dependent histone mRNA 3'-end processing.* EMBO Rep, 2009. **10**(8): p. 894-900.
176. Lee, J.H., et al., *RNF20 Suppresses Tumorigenesis by Inhibiting SREBP1c-PTTG1 Axis in Kidney Cancer.* Mol Cell Biol, 2017.

177. Ren, P., et al., *RNF20 promotes the polyubiquitination and proteasome-dependent degradation of AP-2alpha protein*. Acta Biochim Biophys Sin (Shanghai), 2014. **46**(2): p. 136-40.
178. Buszczak, M., S. Paterno, and A.C. Spradling, *Drosophila stem cells share a common requirement for the histone H2B ubiquitin protease scrawny*. Science, 2009. **323**(5911): p. 248-51.
179. Karpiuk, O., et al., *The histone H2B monoubiquitination regulatory pathway is required for differentiation of multipotent stem cells*. Mol Cell, 2012. **46**(5): p. 705-13.
180. Fuchs, G., et al., *RNF20 and USP44 regulate stem cell differentiation by modulating H2B monoubiquitylation*. Mol Cell, 2012. **46**(5): p. 662-73.
181. Shema, E., et al., *The histone H2B-specific ubiquitin ligase RNF20/hBRE1 acts as a putative tumor suppressor through selective regulation of gene expression*. Genes Dev, 2008. **22**(19): p. 2664-76.
182. Prenzel, T., et al., *Estrogen-dependent gene transcription in human breast cancer cells relies upon proteasome-dependent monoubiquitination of histone H2B*. Cancer Res, 2011. **71**(17): p. 5739-53.
183. Chernikova, S.B., et al., *Deficiency in mammalian histone H2B ubiquitin ligase Bre1 (Rnf20/Rnf40) leads to replication stress and chromosomal instability*. Cancer Res, 2012. **72**(8): p. 2111-9.
184. Zhang, X.Y., et al., *The putative cancer stem cell marker USP22 is a subunit of the human SAGA complex required for activated transcription and cell-cycle progression*. Mol Cell, 2008. **29**(1): p. 102-11.
185. Mannelli, G. and O. Gallo, *Cancer stem cells hypothesis and stem cells in head and neck cancers*. Cancer Treat Rev, 2012. **38**(5): p. 515-39.
186. Szafarowski, T. and M.J. Szczepanski, *Cancer stem cells in head and neck squamous cell carcinoma*. Otolaryngol Pol, 2014. **68**(3): p. 105-11.
187. Satpute, P.S., et al., *Cancer stem cells in head and neck squamous cell carcinoma: a review*. Asian Pac J Cancer Prev, 2013. **14**(10): p. 5579-87.
188. Prince, M.E. and L.E. Ailles, *Cancer stem cells in head and neck squamous cell cancer*. J Clin Oncol, 2008. **26**(17): p. 2871-5.
189. Ben-Porath, I., et al., *An embryonic stem cell-like gene expression signature in poorly differentiated aggressive human tumors*. Nat Genet, 2008. **40**(5): p. 499-507.
190. Okamoto, A., et al., *Expansion and characterization of cancer stem-like cells in squamous cell carcinoma of the head and neck*. Oral Oncol, 2009. **45**(7): p. 633-9.
191. Ailles, L. and M. Prince, *Cancer stem cells in head and neck squamous cell carcinoma*. Methods Mol Biol, 2009. **568**: p. 175-93.
192. Chinn, S.B., et al., *Cancer stem cells: mediators of tumorigenesis and metastasis in head and neck squamous cell carcinoma*. Head Neck, 2015. **37**(3): p. 317-26.
193. Pastrana, E., V. Silva-Vargas, and F. Doetsch, *Eyes wide open: a critical review of sphere-formation as an assay for stem cells*. Cell Stem Cell, 2011. **8**(5): p. 486-98.
194. Spafford, M.F., et al., *Correlation of tumor markers p53, bcl-2, CD34, CD44H, CD44v6, and Ki-67 with survival and metastasis in laryngeal squamous cell carcinoma*. Arch Otolaryngol Head Neck Surg, 1996. **122**(6): p. 627-32.
195. Joshua, B., et al., *Frequency of cells expressing CD44, a head and neck cancer stem cell marker: correlation with tumor aggressiveness*. Head Neck, 2012. **34**(1): p. 42-9.
196. Siddique, H.R. and M. Saleem, *Role of BMI1, a stem cell factor, in cancer recurrence and chemoresistance: preclinical and clinical evidences*. Stem Cells, 2012. **30**(3): p. 372-8.

197. Proctor, E., et al., *Bmi1 enhances tumorigenicity and cancer stem cell function in pancreatic adenocarcinoma*. PLoS One, 2013. **8**(2): p. e55820.
198. Su, Y.J., et al., *Direct reprogramming of stem cell properties in colon cancer cells by CD44*. EMBO J, 2011. **30**(15): p. 3186-99.
199. Boyer, L.A., et al., *Core transcriptional regulatory circuitry in human embryonic stem cells*. Cell, 2005. **122**(6): p. 947-56.
200. Zalzman, M., et al., *Zscan4 regulates telomere elongation and genomic stability in ES cells*. Nature, 2010. **464**(7290): p. 858-U66.
201. Liu, T.J., et al., *Apoptosis induction by E2F-1 via adenoviral-mediated gene transfer results in growth suppression of head and neck squamous cell carcinoma cell lines*. Cancer Gene Ther, 1999. **6**(2): p. 163-71.
202. Ohbo, K., et al., *Modulation of hematopoiesis in mice with a truncated mutant of the interleukin-2 receptor gamma chain*. Blood, 1996. **87**(3): p. 956-67.
203. Adhikary, G., et al., *Identification of a population of epidermal squamous cell carcinoma cells with enhanced potential for tumor formation*. PLoS One, 2013. **8**(12): p. e84324.
204. Leis, O., et al., *Sox2 expression in breast tumours and activation in breast cancer stem cells*. Oncogene, 2012. **31**(11): p. 1354-65.
205. Lu, Y., et al., *Knockdown of Oct4 and Nanog expression inhibits the stemness of pancreatic cancer cells*. Cancer Lett, 2013. **340**(1): p. 113-23.
206. Jiang, J., et al., *Zscan4 promotes genomic stability during reprogramming and dramatically improves the quality of iPS cells as demonstrated by tetraploid complementation*. Cell Res, 2012.
207. Gaspar-Maia, A., et al., *Open chromatin in pluripotency and reprogramming*. Nat Rev Mol Cell Biol, 2011. **12**(1): p. 36-47.
208. Meissner, A., M. Wernig, and R. Jaenisch, *Direct reprogramming of genetically unmodified fibroblasts into pluripotent stem cells*. Nat Biotechnol, 2007. **25**(10): p. 1177-81.
209. Akiyama, T., et al., *Transient bursts of Zscan4 expression are accompanied by the rapid derepression of heterochromatin in mouse embryonic stem cells*. DNA Res, 2015. **22**(5): p. 307-18.
210. Hu, Y. and G.K. Smyth, *ELDA: extreme limiting dilution analysis for comparing depleted and enriched populations in stem cell and other assays*. J Immunol Methods, 2009. **347**(1-2): p. 70-8.
211. van Vlerken, L.E., et al., *EZH2 is required for breast and pancreatic cancer stem cell maintenance and can be used as a functional cancer stem cell reporter*. Stem Cells Transl Med, 2013. **2**(1): p. 43-52.
212. Eyler, C.E. and J.N. Rich, *Survival of the fittest: cancer stem cells in therapeutic resistance and angiogenesis*. J Clin Oncol, 2008. **26**(17): p. 2839-45.
213. Sano, D. and J.N. Myers, *Metastasis of squamous cell carcinoma of the oral tongue*. Cancer Metastasis Rev, 2007. **26**(3-4): p. 645-62.
214. Allegra, E. and S. Trapasso, *Cancer stem cells in head and neck cancer*. Onco Targets Ther, 2012. **5**: p. 375-83.
215. Price, B.D. and A.D. D'Andrea, *Chromatin remodeling at DNA double-strand breaks*. Cell, 2013. **152**(6): p. 1344-54.
216. Park, H.S., et al., *Generation of induced pluripotent stem cells without genetic defects by small molecules*. Biomaterials, 2015. **39**: p. 47-58.

217. Lee, K. and L.S. Gollahon, *ZSCAN4 and TRF1: A functionally indirect interaction in cancer cells independent of telomerase activity*. *Biochem Biophys Res Commun*, 2015. **466**(4): p. 644-9.
218. Schneider, C.A., W.S. Rasband, and K.W. Eliceiri, *NIH Image to ImageJ: 25 years of image analysis*. *Nat Methods*, 2012. **9**(7): p. 671-5.
219. Li, W. and Y. Ye, *Polyubiquitin chains: functions, structures, and mechanisms*. *Cell Mol Life Sci*, 2008. **65**(15): p. 2397-406.
220. Zhu, B., et al., *Monoubiquitination of human histone H2B: the factors involved and their roles in HOX gene regulation*. *Mol Cell*, 2005. **20**(4): p. 601-11.
221. Eidahl, J.O., et al., *Mouse Dux is myotoxic and shares partial functional homology with its human paralog DUX4*. *Hum Mol Genet*, 2016. **25**(20): p. 4577-4589.
222. Dan, J., et al., *Roles for Tbx3 in regulation of two-cell state and telomere elongation in mouse ES cells*. *Sci Rep*, 2013. **3**: p. 3492.
223. Choi, S.H., et al., *DUX4 recruits p300/CBP through its C-terminus and induces global H3K27 acetylation changes*. *Nucleic Acids Res*, 2016. **44**(11): p. 5161-73.
224. Baur, J.A., et al., *Telomere position effect in human cells*. *Science*, 2001. **292**(5524): p. 2075-7.
225. Seto, E. and M. Yoshida, *Erasers of histone acetylation: the histone deacetylase enzymes*. *Cold Spring Harb Perspect Biol*, 2014. **6**(4): p. a018713.
226. Schoeftner, S. and M.A. Blasco, *A 'higher order' of telomere regulation: telomere heterochromatin and telomeric RNAs*. *EMBO J*, 2009. **28**(16): p. 2323-36.
227. Lamarche, B.J., N.I. Orazio, and M.D. Weitzman, *The MRN complex in double-strand break repair and telomere maintenance*. *FEBS Lett*, 2010. **584**(17): p. 3682-95.